Cell Reports
Methods

Article

Targeted mass-spectrometry-based assays enable multiplex quantification of receptor tyrosine kinase, MAP kinase, and AKT signaling

Graphical abstract

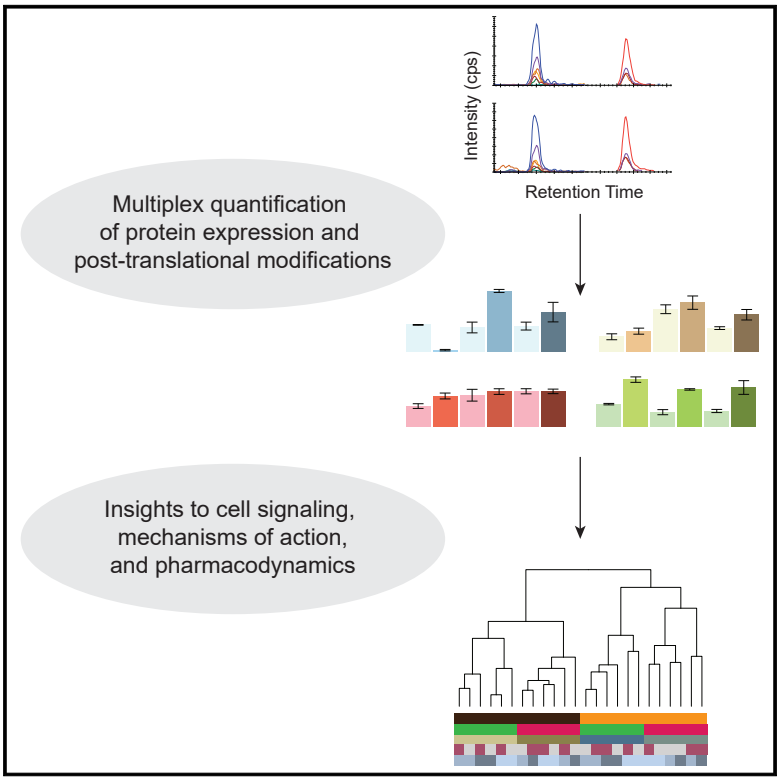

Authors

Jeffrey R. Whiteaker, Kanika Sharma, Melissa A. Hoffman, ..., Steven A. Carr, John M. Koomen, Amanda G. Paulovich

Correspondence

john.koomen@moffitt.org (J.M.K.), apaulovi@fredhutch.org (A.G.P.)

In brief

Whiteaker et al. describe a suite of mass-spectrometry-based assays for quantification of protein expression and phosphorylation in receptor tyrosine kinase, AKT, and MAP-kinase networks. The assays provide a resource for replacing over 60 commonly used cancer signaling and tumor biology western blots with high molecular specificity and quantitative rigor.

Highlights

- Quantitative protein assays are required to understand cancer signaling networks
- We develop a suite of multiplexed mass-spectrometry-based assays
- The assays offer specific and precise quantification of key networks and PTMs
- The assays provide a resource for mechanism-of-action and pharmacodynamic measurements

Whiteaker et al., 2021, Cell Reports Methods *1*, 100015
July 26, 2021 © 2021 The Authors.
https://doi.org/10.1016/j.crmeth.2021.100015

CellPress

Cell Reports Methods

CellPress
OPEN ACCESS

Article

Targeted mass-spectrometry-based assays enable multiplex quantification of receptor tyrosine kinase, MAP kinase, and AKT signaling

Jeffrey R. Whiteaker,[1,10] Kanika Sharma,[2,10] Melissa A. Hoffman,[3,10] Eric Kuhn,[4,10] Lei Zhao,[1] Alexandra R. Cocco,[5] Regine M. Schoenherr,[1] Jacob J. Kennedy,[1] Ulianna Voytovich,[1] Chenwei Lin,[1] Bin Fang,[3] Kiah Bowers,[3] Gordon Whiteley,[6] Simona Colantonio,[6] William Bocik,[6] Rhonda Roberts,[6] Tara Hiltke,[7] Emily Boja,[7] Henry Rodriguez,[7] Frank McCormick,[2,8] Matthew Holderfield,[2,9] Steven A. Carr,[4] John M. Koomen,[3,*] and Amanda G. Paulovich[1,11,*]

[1]Clinical Research Division, Fred Hutchinson Cancer Research Center, Seattle, WA 98109, USA
[2]NCI RAS Initiative, Cancer Research Technology Program, Frederick National Laboratory for Cancer Research, Frederick, MD 21701, USA
[3]Proteomics and Metabolomics Core, Department of Molecular Oncology, and Department of Tumor Biology, Moffitt Cancer Center & Research Institute, Tampa, FL 33612, USA
[4]Broad Institute of Massachusetts Institute of Technology and Harvard, Cambridge, MA 02142, USA
[5]Gillings School of Global Public Health, Kenan-Flagler Business School, University of North Carolina, Chapel Hill, NC 27599, USA
[6]Antibody Characterization Laboratory, Leidos Biochemical Research Inc, Frederick National Laboratory for Cancer Research ATRF, Frederick, MD 21701, USA
[7]Office of Cancer Clinical Proteomics Research, National Cancer Institute, Bethesda, MD 20892, USA
[8]Helen Diller Family Comprehensive Cancer Center, University of California San Francisco, San Francisco, CA 94158, USA
[9]Department of Biology, Revolution Medicines, Inc., Redwood City, CA 94063, USA
[10]These authors contributed equally
[11]Lead contact
*Correspondence: john.koomen@moffitt.org (J.M.K.), apaulovi@fredhutch.org (A.G.P.)
https://doi.org/10.1016/j.crmeth.2021.100015

MOTIVATION A lack of quantitative, multiplexable assays for phosphosignaling limits comprehensive investigation of aberrant signaling in cancer and evaluation of novel treatments. To alleviate this limitation, we sought to develop assays by using targeted mass spectrometry for quantifying protein expression and phosphorylation through the receptor tyrosine kinase, MAPK, and AKT signaling networks. The resulting assays provide a resource for replacing over 60 western blots in examining cancer signaling and tumor biology with high molecular specificity and quantitative rigor.

SUMMARY

A primary goal of the US National Cancer Institute's Ras initiative at the Frederick National Laboratory for Cancer Research is to develop methods to quantify RAS signaling to facilitate development of novel cancer therapeutics. We use targeted proteomics technologies to develop a community resource consisting of 256 validated multiple reaction monitoring (MRM)-based, multiplexed assays for quantifying protein expression and phosphorylation through the receptor tyrosine kinase, MAPK, and AKT signaling networks. As proof of concept, we quantify the response of melanoma (A375 and SK-MEL-2) and colorectal cancer (HCT-116 and HT-29) cell lines to BRAF inhibition by PLX4720. These assays replace over 60 western blots with quantitative mass-spectrometry-based assays of high molecular specificity and quantitative precision, showing the value of these methods for pharmacodynamic measurements and mechanism-of-action studies. Methods, fit-for-purpose validation, and results are publicly available as a resource for the community at assays.cancer.gov.

INTRODUCTION

Cancer signaling plays a key role in tumor biology and has both scientific and clinical relevance to the development and clinical application of targeted therapeutics, especially kinase inhibitors (Gross et al., 2015). Signaling drives cancer growth and proliferation through different protein families, including receptor tyrosine kinases (RTK), mitogen-activated protein kinases (MAPK), the Src homology 2-like serine/threonine-protein kinase B family (AKT), and their upstream and downstream effectors. These pathways play critical roles in cancer formation and progression by altering biological switches in cell signaling networks

This is an open access article under the CC BY-NC-ND license (http://creativecommons.org/licenses/by-nc-nd/4.0/).

(Downward, 2003; Roberts and Der, 2007; Young et al., 2009). For example, RAS is the most frequently mutated oncogene in cancer and plays an important role in cell proliferation. Despite decades of work, therapeutic targeting of RAS has proved challenging, although novel targeting strategies and new drug classes are renewing hope (Khan et al., 2020). A primary goal of the RAS Initiative at the Frederick National Laboratory for Cancer Research is to develop assays for RAS activity, localization, and signaling and to adapt those assays so they can be used for finding new drug candidates to treat cancer (https://www.cancer.gov/research/key-initiatives/ras).

To quantify protein expression and phosphorylation, biologists are currently reliant on established technologies, primarily western blotting (WB) or immunohistochemistry (IHC). WB and IHC are widely used and easily distributed but suffer from many well-known limitations. Specifically, proteins are assessed one at a time (Gown, 2016; Janes, 2015; Kumar et al., 2018; Walker, 2006) in a semi-quantitative fashion susceptible to interferences, and generally cannot be multiplexed. The method is also limited by the lack of highly qualified antibodies for targets of interest (Kumar et al., 2018), poor specificity of many antibodies (Saper, 2009), lot-to-lot variation, and the excessive cost and/or lead time of development, which often relies on a trial-and-error approach to qualify antibodies for an intended assay. A platform capable of standardized, precise, specific, multiplexed quantification of proteins and post-translational modification (PTM) would provide the community with better tools to study basic mechanisms of cell signaling, identify novel drug targets, determine the molecular basis for combination therapies, and help translate relevant findings into clinical use.

Multiple reaction monitoring mass spectrometry (MRM) is a targeted form of proteomics that provides rigorous quantification of proteins and PTMs (Boja and Rodriguez, 2012; Gillette and Carr, 2013; Picotti et al., 2013; Wang et al., 2009) and overcomes limitations associated with conventional immunoassays. The technique has an extensive history of use for quantification of small molecules (Chace and Kalas, 2005; Want et al., 2005) and has been extended to proteins by measuring peptides as stoichiometric surrogates for the protein of interest (Lange et al., 2008). In this approach proteins are digested to peptides, and the peptides are measured by liquid chromatography (LC) coupled to tandem mass spectrometry (LC-MS/MS). The mass spectrometer is tuned to measure specific precursor/fragment ion pairs, termed transitions, which enhance the signal-to-noise ratio (i.e., sensitivity) and confer high specificity. The MRM approach is quantitative through applying isotopically labeled standards that can be spiked into samples at a known concentration. Assays are readily multiplexed by combining multiple MRM transitions into a single MS method. MRM provides near absolute specificity by combining detection of multiple MS/MS fragment ions, alignment of the relative abundance of detected ions with expected ratios from synthetic standards, and alignment of retention times of analyte peptides and internal standards. Furthermore, these measurements allow for detection and avoidance of interferences through the choice of fragment ions to monitor. Finally, the use of standards allows for harmonization across laboratories. The success of the MRM approach has been demonstrated by application to quantification of cancer-associated proteins (Huttenhain et al., 2012) and PTMs (Gerber et al., 2003), use in assessment of multiple components of biological pathways (Chen et al., 2010; Rebecca et al., 2014; Whiteaker et al., 2018), implementation as part of large-scale assay development efforts for hundreds of analytes (Burgess et al., 2014; Kennedy et al., 2014), and validation in inter-laboratory studies (Addona et al., 2009; Kuhn et al., 2012). Furthermore, these MRM-based strategies can be used to identify novel pharmacodynamic biomarkers of kinase inhibition (Jones et al., 2018) or immunomodulatory agents as examples of cancer therapy (Sperling et al., 2019). The direct LC-MRM approach is complemented by enrichment strategies to enable measurement of low-abundance analytes. Enrichment strategies include immobilized metal affinity chromatography (Kennedy et al., 2016) (IMAC) for phosphopeptides and peptide immunoaffinity enrichment (Anderson et al., 2004; Gerber et al., 2003; Ippoliti et al., 2016; Kuhn et al., 2012; Whiteaker et al., 2011) (immuno-MRM, also known as SISCAPA [Anderson et al., 2004]) for specific unmodified and modified peptides using antibodies developed specifically for the MRM target peptides. Like conventional immunoassays, the immuno-MRM approach depends on antibodies with high affinity for the peptide target. However, the near absolute specificity of the mass spectrometer allows for some off-target binding while maintaining high selectivity.

Here, we describe the development, validation, and proof-of-concept application of a suite of MRM-based assays to quantify proteins and phosphosites involved in the RTK, MAPK, and AKT signaling networks. The quantitative assays were developed in three formats: (1) direct LC-MRM (direct-MRM) analysis for expression analysis of high-abundance proteins without enrichment; (2) IMAC enrichment prior to LC-MRM (IMAC-MRM) for quantification of phosphopeptides; and (3) antibody enrichment of unmodified and phosphorylated peptides prior to MRM (immuno-MRM). Assays were characterized in accordance with fit-for-purpose guidelines (Whiteaker et al., 2014, 2016) corresponding to tier 2 level validation (Carr et al., 2014). As a proof of concept, we examined differences in response to BRAF inhibition in melanoma and colorectal cancer cell lines. Targeted inhibitors have been developed against the tumor driver, $BRAF^{V600E}$, which is found in 50% of melanomas (Davies et al., 2002) and 10% of colorectal cancers (Prahallad et al., 2012). BRAF inhibitors have been shown to be effective against 80% of $BRAF^{V600E}$-mutated melanomas, but response rates are just 5% in $BRAF^{V600E}$-mutated colorectal cancer (CRC) (Prahallad et al., 2012). Furthermore, BRAF inhibitors are ineffective in RAS-mutated cells because of a well-described phenomenon: paradoxical activation of ERK1/2 (Cox and Der, 2010, 2012; Holderfield et al., 2014; Poulikakos et al., 2010). Cancer biologists frequently use the BRAF inhibitor (BRAFi), PLX4720, (Tsai et al., 2008), which is a non-clinical tool compound similar to vemurafenib (Bollag et al., 2010) to investigate the signaling underlying this unmet medical need; PLX4720 is highly effective in $BRAF^{V600E}$-driven melanomas (Flaherty et al., 2010) but elicits only weak therapeutic response in $BRAF^{V600E}$-mutated CRCs (Prahallad et al., 2012). Therefore, we have chosen this test case for our assay platforms, given that these phenomena have been well characterized in multiple cell line models providing the capability to verify the results of these MRM-based

CellPress
OPEN ACCESS

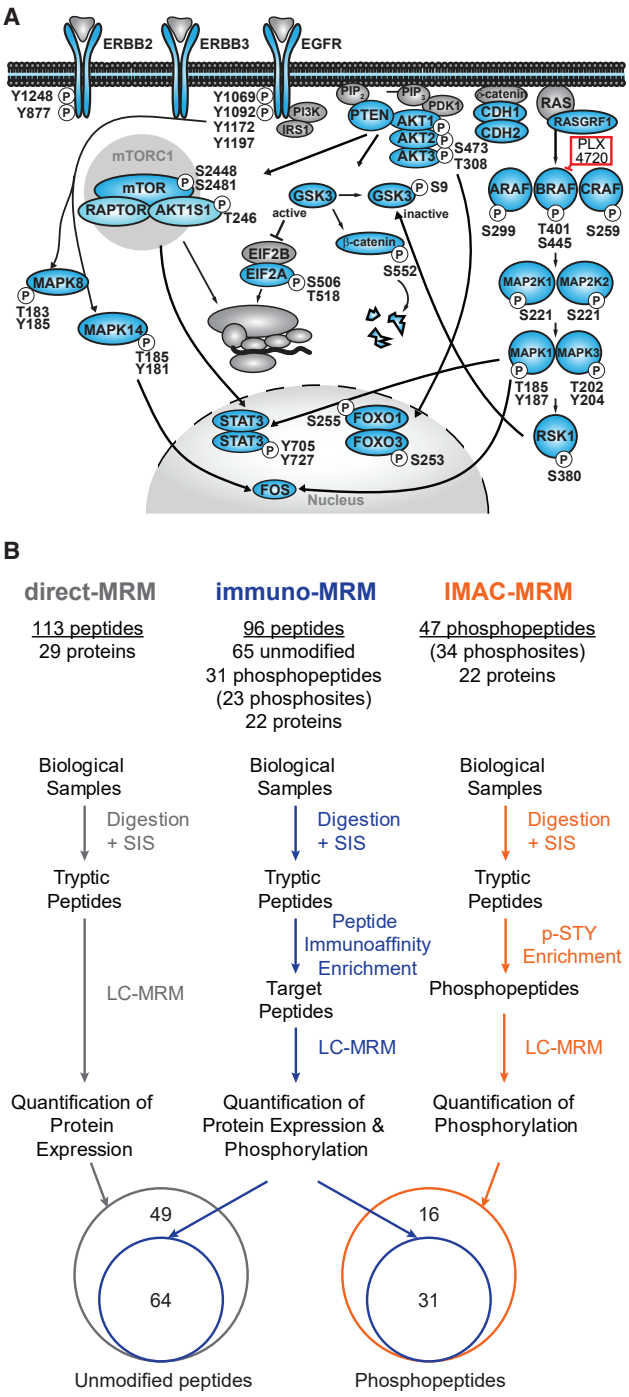

Figure 1. Development of quantitative assay panels targeting cancer signaling to promote cellular growth and proliferation

(A) RTK, MAPK, and AKT signaling networks were targeted for MS-based assay development to quantify expression and phosphorylation of proteins that drive cellular growth and proliferation in cancer. Proteins targeted by the MRM assay panels are colored blue; additional signaling nodes not included in the assay panel are shown in gray; the BRAF inhibitor, PLX4720, is shown in red.

(B) The different sample processing workflows culminate in LC-MRM of tryptic peptides using a spiked-in stable isotope-labeled standard (SIS) for each analyte. Direct-MRM targets higher-abundance proteins, IMAC-MRM targets phosphopeptides (i.e., pSTY) for enrichment prior to MRM, and immuno-MRM uses custom monoclonal antibodies for peptide immunoaffinity enrichment of selected unmodified and phosphorylated peptides. Peptides measured in common between methods are shown in the Venn diagrams. The protocols, reagents, and assay characterization data, as well as demonstration of utility of the methods for pharmacodynamic and proof-of-mechanism studies, are presented in this article.

assays. Finally, to enable distribution in the research community, the information and resources needed to implement the assays (e.g., standard operating protocols, metrics, instrument parameters, and antibody reagents) are publicly available through the National Cancer Institute's Clinical Proteomics Tumor Assessment Consortium (CPTAC) Assay Portal (assays.cancer.gov) (Whiteaker et al., 2014, 2016), and the CPTAC Antibody Portal (antibodies.cancer.gov). Application of these assays will aid exploration in aspects of cellular signaling in cancer biology and targeted therapy.

RESULTS

Target selection and MRM assay development

Proteins and phosphorylation sites that sustain cell growth and proliferation in the RTK, MAPK, and AKT signaling networks were identified as targets for assay development by members of the US National Cancer Institute's RAS Initiative (https://www.cancer.gov/research/key-initiatives/ras; see Table S1 and Figure 1A). Selecting from this target list, we developed MRM-based assay platforms to assess key nodes in cancer signaling as a proof of concept in an initial step toward a comprehensive panel to elucidate tumor biology, assist with development of targeted therapy, and streamline assay implementation for companion diagnostics. Peptides amenable to MS were identified by mining existing LC-MS/MS proteomic and phosphoproteomic datasets (Bhowmick et al., 2018; Kusebauch et al., 2016; Remily-Wood et al., 2011; Whiteaker et al., 2014, 2016), including data from breast, ovarian, and CRC tissues, cancer cell lines, and public databases, for empirical evidence of LC-MS/MS detectability. After ranking peptides on the basis of observational, chemical, and physical properties, further review focused on known mutation sites by using CBioPortal (Cerami et al., 2012), PTMs by using PhosphoSitePlus (Hornbeck et al., 2012, 2019), and assessment of potential interference by using the *in silico* Peptide Interference Predictor (Remily-Wood et al., 2014).

On the basis of this information, 167 peptides (including multiple peptides per protein) were selected for assay development, representing 29 proteins and 34 phosphorylation sites. Peptide sequences selected for assay development are listed in Table S1. Several MRM-based multiplexed assay panels were developed for the selected peptides, including one direct-MRM, one IMAC-MRM, and two immuno-MRM, which all require upfront protein digestion with trypsin and use spiked-in stable isotope standard (SIS) peptides for precise relative quantification. The three assay types are distinguished by the extent and type of enrichment performed prior to measurement (Figure 1B). The direct-MRM assay measures peptides present in a tryptic digest without enrichment or fractionation prior to analysis; this assay is

suitable for measurement of expression of moderately to highly abundant proteins. IMAC-MRM enriches phosphopeptides by using immobilized metal affinity chromatography prior to LC-MRM analysis, so only phosphopeptides will be detected and quantified. Immuno-MRM uses anti-peptide antibodies (Schoenherr et al., 2019) for enrichment prior to LC-MRM and is applicable for quantifying expression of high- and low-abundance proteins as well as phosphopeptides. For the two immuno-MRM assay panels, the monoclonal antibodies developed specifically for this purpose have already been characterized (Schoenherr et al., 2019).

Fit-for-purpose validation was performed to characterize each assay panel; results for individual peptide performance are reported in Table S2 and a summary of validation data are available in Figures S1A–S1E. In total, we validated assays targeting 113 unmodified peptides by direct-MRM, 47 phosphopeptides by IMAC-MRM, and 96 (unmodified and phosphorylated) peptides by immuno-MRM (Figure 1B). Each assay group had a median linear response range of over three orders of magnitude. The median lower limit of quantification (LLOQ) was 200 fmol/mg (or 200 amol/μg) for direct-MRM, 12.5 fmol/mg for IMAC-MRM, and 6.12 fmol/mg for immuno-MRM. Finally, percent coefficient of variation (%CV) from characterization of within-day repeatability (intra-assay %CV) were 2%, 2%, and 9%, and the between-day repeatability (inter-assay %CV) were 3%, 2%, and 18% for the direct-MRM, IMAC-MRM, and immuno-MRM assays, respectively. Assay portability of the immuno-MRM platform is shown in Figure S1F by an inter-laboratory evaluation at three different sites showing good correlation ($R^2 > 0.92$) and agreement ($1.09 > \text{slope values} > 0.79$).

The MRM methods are capable of quantifying cell signaling dynamics

We conducted proof-of-principle experiments to demonstrate application of the quantitative multiplexed assays in profiling changes in protein expression and phosphorylation in melanoma and CRC cell lines harboring either BRAF or RAS mutations ± PLX4720 treatment. BRAF-mutated melanomas are sensitive to the initial treatments of PLX4720; in BRAF-mutated CRC, epidermal growth factor receptor (EGFR) signaling reactivates the MAPK pathway (Tse and Verkhivker, 2016). In RAS-mutated melanomas and CRC, PLX4720 paradoxically activates the MAPK pathway through CRAF, leading to excessive proliferation and rendering PLX4720 ineffective. We used four cell lines, including BRAF inhibitor-sensitive A375 ($BRAF^{V600E}$) and inhibitor-resistant SK-MEL-2 ($NRAS^{Q61R}$) melanoma cell lines, as well as resistant HT-29 ($BRAF^{V600E}$) and HCT-116 ($KRAS^{G13D}$) (Ahn et al., 2015; Corcoran et al., 2012) colon cancer cell lines (CCLE Drug Data, 2015; Barretina et al., 2012), as a test case in drug sensitivity and resistance based on their response to BRAF inhibition with 3 μM PLX4720. We confirmed the differential sensitivity of A375 ($BRAF^{V600E}$ melanoma), HT-29 ($BRAF^{V600E}$ CRC), HCT-116 ($KRAS^{G13D}$ CRC), and SK-MEL-2 ($NRAS^{Q61R}$ melanoma) to PLX4720 by measuring proliferation in a 72-h assay (Figure S2A). Mirroring expectations of known biology and clinical observations, $BRAF^{V600E}$ melanoma cells (A375) demonstrated greater sensitivity to PLX4720 than $BRAF^{V600E}$ CRC cells (HT-29), and the RAS-mutant melanoma and CRC cells (SK-MEL-2 and HCT-116, respectively) showed resistance to PLX4720. Protein from whole-cell lysates (treated with DMSO vehicle control or PLX4720, harvested at 1.5, 24, and 48 h of drug exposure; two biological replicates) were proteolyzed with trypsin, and peptides were quantified by direct-MRM or used for enrichment prior to IMAC- or immuno-MRM analysis (data are provided in Table S3). Most peptides were detected above the LLOQ in more than half of the samples (60 out of 113 peptides for direct-MRM, 23 out of 47 phosphopeptides for IMAC-MRM, and 80 out of 96 unmodified and phosphopeptides for immuno-MRM). For comparison between assay platforms, 48 out of 64 unmodified peptide signals were above LLOQ in both direct-MRM and immuno-MRM assays, while 18 out of 31 phosphopeptide signals were detected above LLOQ by both IMAC-MRM and immuno-MRM assays (Table S4 and Figure S2B). Overall, widespread profiling of protein expression and phosphorylation was obtained using the MRM methods, demonstrating efficient multiplexed measurement of cellular signaling.

To examine the breadth of information obtained by the multiplexed assay, we analyzed expression levels from each assay by unsupervised (Figure 2) and supervised clustering (Figure S3). As expected, unsupervised clustering of the MRM data grouped samples according to cell line and mutation status. Furthermore, the peptides from the same protein were classified together. In addition, aspects of known biology could also be observed; for example, E-cadherin (CADH1) was quantified at higher levels in CRC cells that are epithelial in nature, whereas N-cadherin (CADH2) was observed at higher levels in melanomas that are mesenchymal (Figures 2A and 2C). Baseline differences in protein expression and phosphorylation (Figure 2) could also be used to distinguish the cell lines (e.g., AKT3 is expressed more highly in melanoma than in CRC cell lines, GSK3B is expressed at the highest levels in SK-MEL-2 cells, EGFR phosphorylation is higher in CRC than these melanoma cell lines) and to differentiate RAS and BRAF mutant cells (e.g., MP2K1 or MEK1 expression is higher in BRAF than in RAS mutant cell lines).

Multiplexed quantitation of protein expression and phosphorylation elucidate response to PLX4720 treatment

To further demonstrate the utility of the multiplexed assay and examine the pharmacodynamic profiling of the activation of growth and proliferation signaling, we plotted the relative expression of unmodified and phosphorylated peptides for several specific relevant targets determined by MRM-based assays for comparison with confirmatory WB in Figure 3. These targets were selected to demonstrate the effectiveness of the quantitative, multiplexed assay in examining central nodes of MAPK (RAS-RAF-MEK-ERK) signaling as well as proteins and phosphorylations involved in previously published mechanisms of BRAFi resistance (e.g., EGFR/ERBB activation, increased CRAF activation, and AKT signaling). A decrease in p-$ERK^{T202/Y204}$ was observed in A375 at 1.5 h with a rebound of phosphorylation at later time points because of rewired ERK1/2 (MAPK1/MAPK3) signaling after PLX4720 treatment that gives rise to resistance (Lito et al., 2012). Consistent with the proliferation data, HT-29 cells showed little change of p-$ERK^{T202/Y204}$ and were unresponsive to PLX4720 at 1.5 h, although shorter time points do show

CellPress
OPEN ACCESS

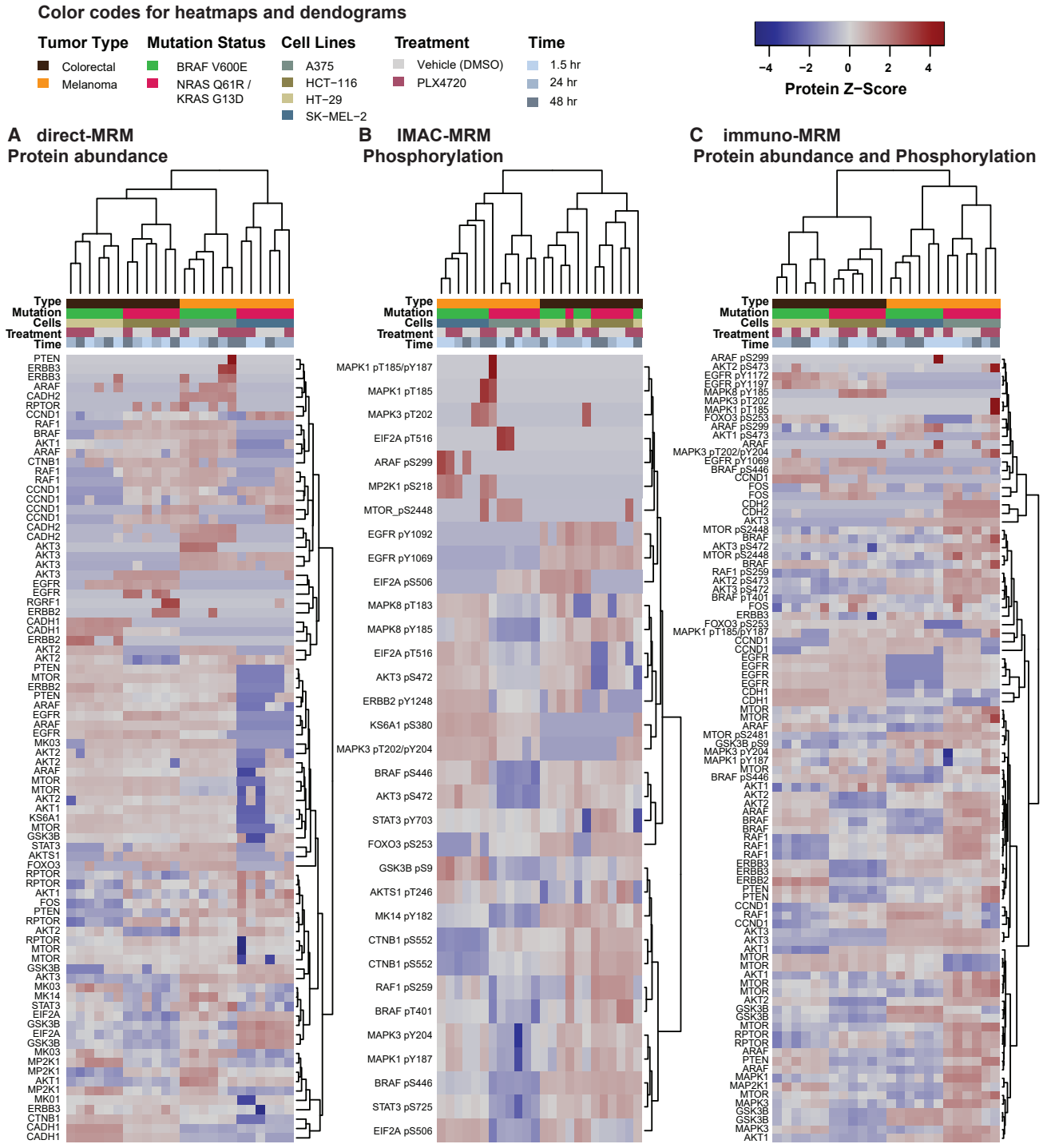

Figure 2. Unsupervised clustering of quantitative MRM data groups primarily by biological differences in cell types

(A–B) Unsupervised clustering of protein expression measured by direct-MRM (A), phosphorylation measured by IMAC-MRM (B), and protein expression and phosphorylation measured by immuno-MRM (C) show that protein expression and phosphorylation predominantly cluster by cell line with secondary clusters grouped by response to PLX treatment. Row heatmap values are *Z* score of the median response for each peptide analyte using the $\log_2$ transformed peak area ratio (light/heavy) values from the MRM data (n = 2 biological replicates); missing values were imputed with LLOQ values.

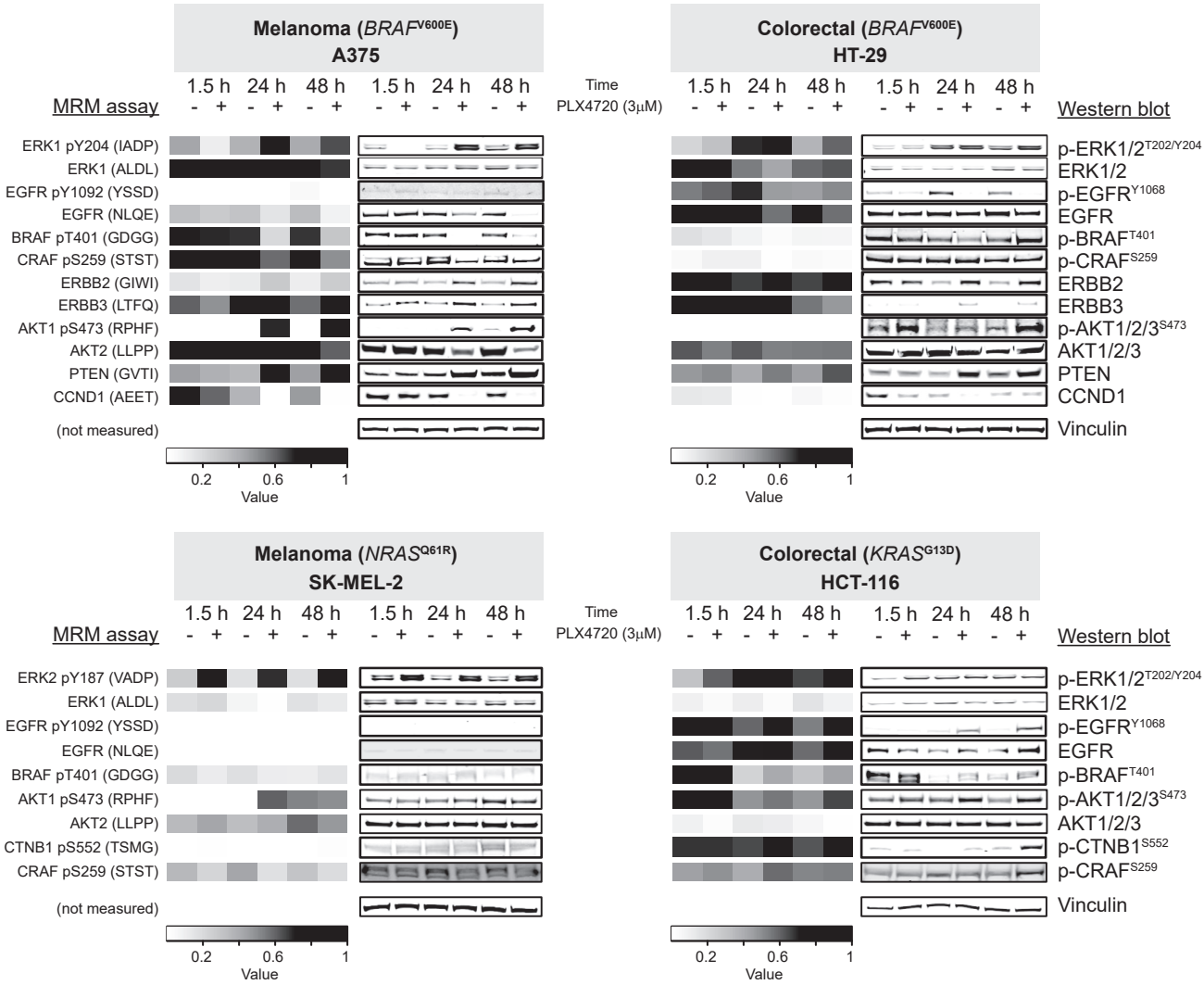

Figure 3. MRM assays show quantitative changes in signaling in melanoma and colorectal cancer cell lines after PLX4720 treatment

Heatmaps of selected quantitative MRM measurements of proteins and phosphosites to examine central nodes of MAPK (RAS-RAF-MEK-ERK) signaling and demonstrate previously published mechanisms of BRAFi resistance in four cancer cell lines. MRM results shown are from immuno-MRM assays with the exceptions of p-EGFR^{Y1092} and p-CTNB1^{S552} (which are IMAC-MRM results). For MRM assays, p-AKT1^{S473} and AKT2 peptide LLPP were chosen for correlation with pan AKT1/2/3 western blots (WB). Each cell in the heatmap is colored according to normalized values for individual analytes across all samples. The quantitative values were correlated with analysis by WB (STAR Methods). Analyte nomenclature was based on the sequence of the peptide analyzed by MRM (left side, "MRM assay" label) and the reported WB antibody specificity (right side, "Western blot" label). Vinculin was used as a loading control for WB. Bar plots are the mean of duplicate biological replicates. Error bars show the range of duplicate biological replicates.

mitigation of signaling by decreases in p-ERK$^{T202/Y204}$ (data not shown). BRAF^{V600E} CRCs are known to be unresponsive to PLX4720 when compared with BRAF^{V600E}-mutated melanomas (Corcoran et al., 2012; Prahallad et al., 2012). The levels of p-EGFR^{Y1092} (position Y1092 in full-length EGFR corresponds to Y1068 after removal of 24 amino acids from the N terminus during processing) in A375 were found to be low (because melanomas typically express low levels of EGFR) (Corcoran et al., 2012; Prahallad et al., 2012); however, p-EGFR^{Y1092} decreased in HT-29 at later time points, indicating that EGFR was not driving resistance in this model. Phosphorylation of BRAF^{T401} also decreased in A375 when compared with HT-29 (Ritt et al., 2010). ERBB2 and ERBB3 have been previously implicated in resistance mechanisms in melanomas treated with RAF/MEK inhibitors and are observed to be upregulated in both A375 and HT-29. This observation highlights non-EGFR RTK-based resistance mechanisms in both melanomas and CRCs (Abel et al., 2013; Herr et al., 2018). Furthermore, p-AKT1/2/3^{S473} activation, likely driven by Rictor/MTOR activation (Sarbassov et al., 2005), was also prevalent in both cell lines (Gopal et al., 2010), and activation of the p-AKT1^{T308} site was observed at 48 h in both cells after PLX treatment (Table S3), consistent with expectations (Espona-Fiedler et al., 2012; Homsi et al., 2009). Of note, PTEN expression increased at later time points in both BRAF-mutated cell lines

CellPress
OPEN ACCESS

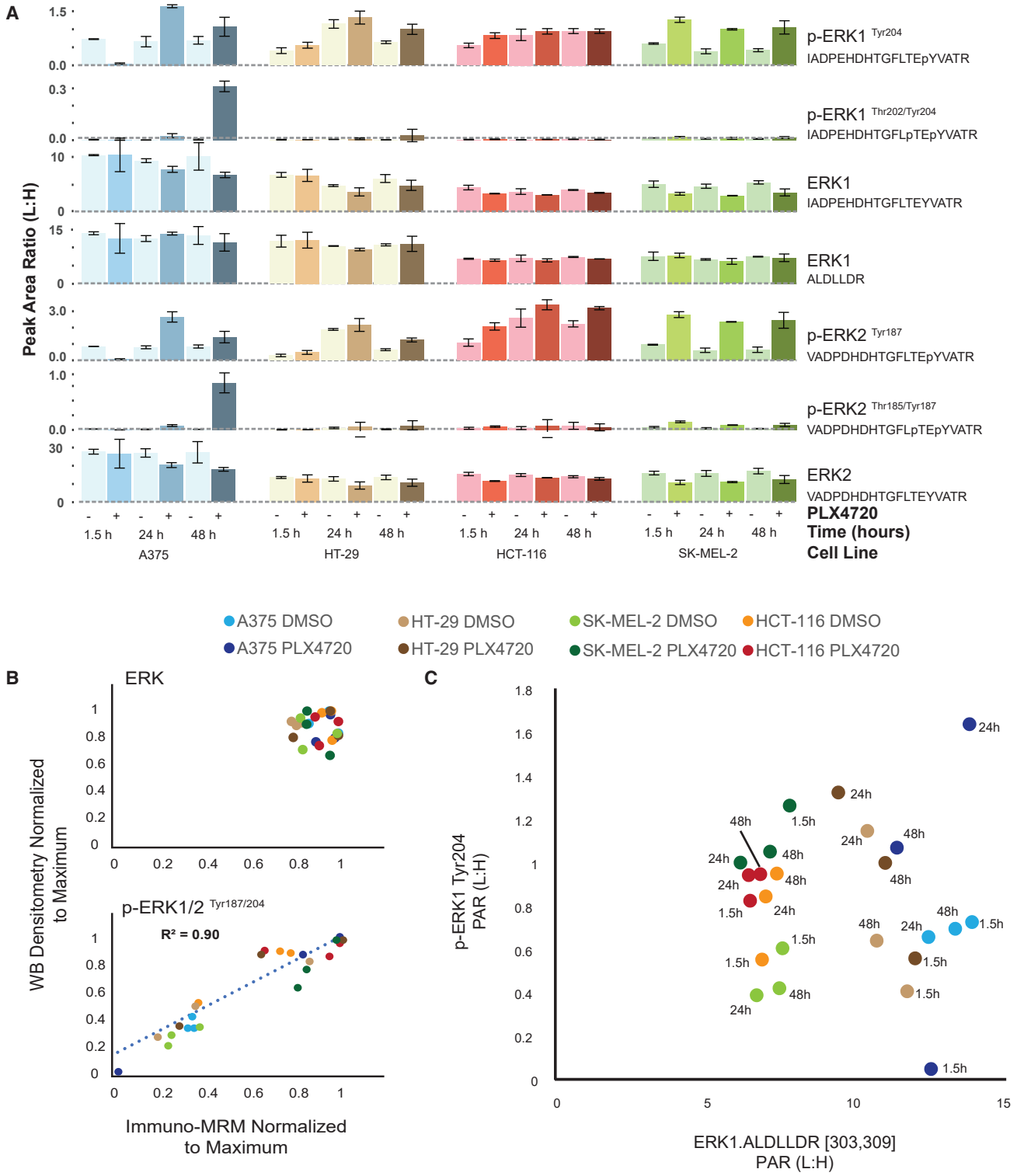

Figure 4. Quantitation of paradoxical ERK1/2 activation after PLX4720 treatment in colorectal cancer and melanoma cell lines illustrates the molecular detail accessible through immuno-MRM measurements

(A) Relative quantitation of ERK1/2 peptides are plotted as mean peak area ratio (PAR) comparing the light endogenous with the heavy internal standard in cell lines ± PLX4720. Error bars show the range of duplicate biological replicates. Dotted line shows the approximate lower limit of quantification (LLOQ).

(legend continued on next page)

(Figure 3); PTEN is required to upregulate Bcl-2-like protein 11 (i.e., BIM) to cause BRAFi-driven apoptosis in melanoma (Paraiso et al., 2011). As expected, the recovery of Cyclin D1 (CCND1) levels in HT-29 at the 48-h time point highlights the difference in sensitivity between A375 and HT-29 (Diao and Chen, 2007). Overall, our MRM-based results indicate the molecular basis for $BRAF^{V600E}$ melanoma (A375) sensitivity to PLX4720 compared with the lesser effect on $BRAF^{V600E}$-mutated CRC (HT-29) and show signaling effects consistent with previous reports (Corcoran et al., 2012; Lee et al., 2010; Prahallad et al., 2012).

Similar observations were made in the RAS-mutated cell lines, HCT-116 and SK-MEL-2 (Figure 3). Phosphorylation of $EGFR^{Y1092}$ and total EGFR both increased in HCT-116 cells. As expected, we were unable to measure the expression of EGFR in SK-MEL-2 cells, consistent with low expression levels of EGFR in melanomas (Corcoran et al., 2012; Prahallad et al., 2012). Phosphorylation of $BRAF^{T401}$, which decreases CRAF binding and results in negative feedback regulation by ERK1/2, was increased in HCT-116 cells. HCT-116 not only had EGFR-dependent MAPK activation but also an increase in p-AKT1/2/3^{S473} caused by RAS-dependent phosphatidylinositol 3-kinase (PI3K)/AKT activation (Figure 3). The activation of p-AKT1/2/3^{S473} in HCT-116 was associated with an induction of p-$CTNNB1^{S552}$, which promotes tumor invasion (Fang et al., 2007); this result is consistent with the increased aggressiveness of RAS-mutant tumors after BRAF inhibition. The protein expression pattern in HCT-116 shows that there are multiple resistance mechanisms occurring in RAS-mutated CRC, which are absent in melanomas. Our data derived from immuno-MRM assays were consistent with WB carried out in parallel and similar to previously published literature, which demonstrate that PLX4720 paradoxically activates p-$ERK^{T202/Y204}$ signaling in both RAS-mutated SK-MEL-2 melanoma and HCT-116 CRC, causing resistance to BRAFi (Holderfield et al., 2014). Furthermore, these results integrate the outcomes of several previous studies and demonstrate the effectiveness of measuring protein expression and phosphorylation for multiple targets by using MRM assays, demonstrating the utility of the MRM-based methods for pharmacodynamic and mechanism-of-action studies, as well as defining mechanisms of drug resistance that alter cell signaling.

MRM results expand the understanding of protein regulation and phosphorylation involved in PLX4720 resistance

The quantitative nature and high specificity of MRM assays offer additional molecular details, as exemplified by analyzing phosphorylation of ERK1/2. Using the specificity of the MRM assays (Figure S4), individual measurements of the monophosphorylated and doubly phosphorylated ERK peptides provide molecular insight into the activation of this kinase. For example, in the case of ERK1/2, unmodified peptides quantifying protein expression show relatively little change, indicating that activity is driven through changes in phosphorylation. Immuno-MRM data are presented, but direct-MRM measurements of protein ERK protein expression and IMAC-MRM measurements of ERK1/2 phosphotyrosine measurements strongly correlate with the immuno-MRM results. Specificity of each phosphosite is conferred through chromatographic separation, detection of internal standard peptides, and consistent fragment ion relative intensities. We find phosphorylation predominantly occurs at the p-Y204/Y187 sites on ERK1/2 (Figure 4A). The p-T sites were only detected at 48 h after exposure to PLX4720. Likewise, for the A375 cells, the doubly phosphorylated peptides also show an increase at 48 h, indicating hyperphosphorylation of the ERK1/2 active sites. This phosphorylation pattern is consistent with previous results (Lee et al., 2019), showing that tyrosine phosphorylation is critical for ERK activation. WB results correlate with the immuno-MRM measurements (Figure 4B), showing consistent trends in the increase of p-$ERK^{T202/Y204}$ phosphorylation compared with DMSO controls. Although the antibody for WB might recognize all phosphorylated forms of ERK1/2, the MRM data quantify each phosphopeptide separately. The additional molecular detail afforded by the MRM assays confirms that tyrosine phosphorylation is the dynamic driving factor in ERK activation and that threonine phosphorylation plays a supporting role. This is further illustrated by examining the relative quantitative relationship of total protein expression and phosphorylation between the cell lines, shown in Figure 4C, which provides insights into the changes in ERK signaling in BRAFi-sensitive and -resistant cells. A375 cells show little change with DMSO, but a significant decrease in signaling at 1.5 h with paradoxical signaling at 24 h that is sustained at 48 h after treatment. All other cell lines show increased p-ERK after BRAF inhibition. Although expression levels differed approximately 2-fold between the cell lines, the activated levels of phosphorylated p-ERK were similar. Furthermore, phosphorylation levels increased more compared with the total expression level of ERK1.

DISCUSSION

In this study, we present methods for MRM-based assays that can be used as a resource for the precise relative quantification of protein expression and signaling in growth and proliferation. The procedures, application notes, and performance data for each of the multiplex MRM assays described here are publicly available through CPTAC's Assay Portal (assays.cancer.gov), and the monoclonal antibodies (Schoenherr et al., 2019) are available via the Antibody Portal (antibodies.cancer.gov) (see Table S1 for assay and antibody identifiers). These fit-for-purpose validated quantitative assays offer advantages over conventional antibody-based forms of protein quantitation (e.g., WB, IHC). For example, MS confirms the specific sequence of the peptide derived from the protein (i.e., the analyte is measured

(B) Densitometry values from western blots (WB) of ERK1/2 expression and phosphorylation in the same cell lysates were used for correlation with immuno-MRM analysis.

(C) The relative levels of total protein expression, plotted as the PAR for the peptide ALDLLDR, are related to levels of the phosphorylated p-$ERK1^{Tyr204}$. The amino acid residue numbers of the peptides within the protein are shown in brackets. Samples are color-coded according to cell line and ±PLX4720 in the key at the top of the panel; data were labeled with time point.

directly and there is no secondary detection/amplification step). Additionally, spiked-in SIS peptides control for some preanalytical variations and facilitate transferability of the assays across laboratories and over time (e.g., quantitation of proteins in different sample types analyzed in different batches). Finally, the assays are multiplexed, performing the equivalent of 63 WBs (for 29 proteins and 34 phosphorylation sites) from the same sample in a single experiment.

Another advantage of the MRM approach is in measuring phosphorylated and non-phosphorylated forms with a multiplexed assay. We demonstrate this utility by showing relative measurements of ERK1/2 protein and phosphoprotein expression. Absolute quantitative conclusions about phosphorylation stoichiometry must be made with caution, however, given that phosphosites can be clustered, not all possible phospho-isoforms might be detected, and phosphorylation near cleavage sites can affect trypsin digestion. If multiple isoforms of the analyte peptide exist, each corresponding mass must be targeted separately in the MRM assay to quantify site occupancy. Thus, the MRM-based assays provide precise relative quantification of the reproducibly recovered tryptic peptide analyte(s) targeted by the MRM method, and further quantitative validation is necessary to provide absolute quantitation of phosphosite stoichiometry.

The assays were developed in three formats: direct-MRM, IMAC-MRM, and immuno-MRM. As expected, each format has its strengths and weaknesses regarding the analytes detected and resources required for implementation. This dataset provides indication of which proteins might require enrichment in future studies. Direct-MRM offers the most straightforward approach to measuring protein expression with the smallest sample requirements and least sample-handling steps. However, it is limited to measurement of higher-abundance proteins, whereas enrichment is required for low-abundance targets and phosphorylated peptides. IMAC-MRM offers the ability to reproducibly measure phosphorylation without target-specific reagents but is limited to a subset of the phosphoproteome and might require additional fractionation to increase recovery of specific phosphopeptides or reduce interference. Immuno-MRM can measure both unmodified and phosphorylated peptides in a single assay and is capable of the highest sensitivity of the three, as it is not limited by sample input amounts and the antibodies provide 10^2- to 10^4-fold enrichment of the target. Unless an applicable antibody already exists (Schoenherr et al., 2016), costs and lead time for developing immuno-MRM assays are greater than for direct- or IMAC-MRM assays, which do not require reagents for target-specific enrichment. As we have demonstrated in this approach using multiple forms of enrichment coupled with MRM, the main limitation to developing an MRM assay is the availability of a peptide that is amenable to analysis by MS and the abundance of the peptide in the specimen of interest.

We demonstrated the application of the multiplexed MRM assay resource for pharmacodynamic and mechanism-of-action studies. As predicted, both RAS-mutated cells, HCT-116 and SK-MEL-2, hyperactivated the MAPK pathway by increasing p-ERK1/2$^{T202/Y204}$. HCT-116 presented a robust multi-mechanism feedback induction by activating both p-EGFR^{Y1092} and p-AKT1/2/3^{S473}, suggesting that RAS-dependent PI3K activation also contributes to PLX4720 resistance. MAPK hyperactivation and subsequent drug resistance was also observed after longer-term drug exposures in BRAF^{V600E}-mutated A375 and HT-29 cell lines. Although low expression prevented detection of EGFR hyperactivation (Corcoran et al., 2012), we did observe upregulation of other RTKs, including ERBB2 and ERBB3 in A375 (Abel et al., 2013) and HT-29 (Herr et al., 2018), supporting a model of ERBB-mediated BRAF inhibitor resistance by reactivating the MAPK and PI3K pathways in these BRAF-mutated cell lines.

Combination therapy has taken center stage in targeting acquired resistance in the clinic. Melanoma and CRC are both complex and heterogeneous diseases, and acquired resistance to targeted therapeutics might be inevitable. Therefore, multiplexed assays such as these provide a way to encompass multiple upstream and downstream signaling network members in a quantitative evaluation of protein expression and phosphorylation during drug treatment to find novel synergistic combinations. Multiple clinical trials are ongoing with the goal of chronically inhibiting BRAF activity while vertically targeting compensatory mechanisms. Although the dual inhibition treatment strategies were not evaluated as part of this study, our assays can provide support for the clinical strategies combining BRAFi + MEKi, BRAFi + HSP90i (Eroglu et al., 2018), BRAFi + PI3Ki, and BRAFi + ERBBi therapies for treatment of BRAF-driven melanomas and CRC (Lee et al., 2010; Lito et al., 2012) and other emerging targeted therapies for RAS-driven tumors.

Moving forward, this assay resource could be expanded to further increase its utility in assessing cancer signaling in the Ras-Raf-MEK-ERK pathway. For example, assays to quantify the DUSP4 and Gab2 proteins could be added to further study signaling in drug-resistant cell lines. Expansion of the assay platform to include reporters for downstream effectors (e.g., changes in cancer metabolism) could provide more links between this panel and cancer phenotypes linked to drug sensitivity or therapeutic resistance. Additional peptides corresponding to other relevant proteins not pursued for assay development in this study are available in Table S1. Other additions to the assay resource could address additional phosphorylation sites on these target proteins, those biologically significant phosphosites that were less amenable to the standard MS workflow (because the sites of interest were in tryptic peptides that were either too small or too large for LC-MS/MS analysis), and those phosphosites where we developed an assay but were unable to measure endogenous expression levels. Modifications to the standard sample processing, such as use of alternative enzymes for digestion, would be necessary to optimize recovery of these phosphosites, allowing expansion of the panel to more phosphosites of interest.

In summary, we have described the development of MRM-based targeted assays for a panel of biologically important proteins and their key phosphosites relevant to targeted cancer therapy. These experiments probing resistance mechanisms in cell lines illustrate the utility of this assay resource by replacing over 60 WBs in examining cancer signaling and tumor biology with high molecular specificity and quantitative rigor, and

demonstrate the value of this assay resource for pharmacodynamic measurements and mechanism-of-action studies.

Limitations of the study

Detection of the targeted analytes depends on expression levels and relative response in the mass spectrometer. The method is most likely to succeed where there is sufficient material available for analysis and phosphorylated proteins are appropriately preserved. For analysis of low-abundance targets, or using limited material, the described enrichment methods are most appropriate. To improve likelihood of detection, increasing the amount of input material might be necessary. Special attention to preanalytical variables (e.g., sample collection, preservation, and lysis conditions) is helpful for minimizing changes in phosphorylation status due to phosphatase activity and/or degradation. When addressed, these considerations make the methods applicable to a variety of applications. In addition to the pharmacodynamic and mechanism-of-action studies demonstrated herein, a broad utility in measuring protein expression and phosphorylation is possible using the assays, including biomarker studies, confirmation of expression, and differential proteomics studies.

STAR★METHODS

Detailed methods are provided in the online version of this paper and include the following:

- KEY RESOURCES TABLE
- RESOURCE AVAILABILITY
  - Lead contact
  - Materials availability
  - Data and code availability
- EXPERIMENTAL MODEL AND SUBJECT DETAILS
  - Cell lines
- METHOD DETAILS
  - Proliferation assays
  - Western blot analysis
  - Peptide selection criteria
  - Enzymatic digestion
  - Peptide immunoaffinity enrichment
  - Liquid chromatography multiple reaction monitoring mass spectrometry
  - Fit-for-purpose assay validation
  - Data analysis
- QUANTIFICATION AND STATISTICAL ANALYSIS

SUPPLEMENTAL INFORMATION

Supplemental information can be found online at https://doi.org/10.1016/j.crmeth.2021.100015.

ACKNOWLEDGMENTS

This project was funded the NCI CPTAC (nos. U24CA160034 and U01CA214114), the NCI RAS Initiative through contracts managed by Leidos (HHSN261200800001E to A.G.P. and S.A.C. and 14x270 to J.M.K.), and the NCI Cancer Research Specialist program (R50CA211499 to J.R.W.). The Moffitt Proteomics & Metabolomics Core is supported as part of an NCI-designated Comprehensive Cancer Center (P30-CA076292) and by the Moffitt Foundation. The authors thank Paul Ippoliti for his contribution in preparation and analysis of samples and reagents.

AUTHOR CONTRIBUTIONS

Conceptualization, A.G.P., J.M.K., and S.A.C.; methodology, A.G.P., J.M.K., S.A.C., and M.H.; investigation, J.R.W., K.S., M.A.H., E.K., L.Z., A.R.C., J.J.K., U.V., B.F., K.B., and S.C.; resources, R.M.S., U.V., and R.R.; data curation, C.L.; Writing – original draft, J.R.W., K.S., J.M.K., M.A.H., and E.K.; supervision, G.W., W.B., T.H., E.B., H.R., F.M., M.H., S.A.C., J.M.K., and A.G.P.; funding acquisition, J.R.W., S.A.C., J.M.K., and A.G.P.

DECLARATION OF INTERESTS

The authors declare no competing interests.

Received: November 3, 2020
Revised: February 16, 2021
Accepted: May 7, 2021
Published: June 14, 2021

REFERENCES

Abel, E.V., Basile, K.J., Kugel, C.H., 3rd, Witkiewicz, A.K., Le, K., Amaravadi, R.K., Karakousis, G.C., Xu, X., Xu, W., Schuchter, L.M., et al. (2013). Melanoma adapts to RAF/MEK inhibitors through FOXD3-mediated upregulation of ERBB3. J. Clin. Invest *123*, 2155–2168.

Addona, T.A., Abbatiello, S.E., Schilling, B., Skates, S.J., Mani, D.R., Bunk, D.M., Spiegelman, C.H., Zimmerman, L.J., Ham, A.J., Keshishian, H., et al. (2009). Multi-site assessment of the precision and reproducibility of multiple reaction monitoring-based measurements of proteins in plasma. Nat. Biotechnol. *27*, 633–641.

Ahn, J.H., Han, B.I., and Lee, M. (2015). Induction of resistance to BRAF inhibitor is associated with the Inability of Spry2 to Inhibit BRAF-V600E activity in BRAF mutant cells. Biomol. Ther. (Seoul) *23*, 320–326.

Anderson, N.L., Anderson, N.G., Haines, L.R., Hardie, D.B., Olafson, R.W., and Pearson, T.W. (2004). Mass spectrometric quantitation of peptides and proteins using stable isotope standards and capture by anti-peptide antibodies (SISCAPA). J. Proteome Res. *3*, 235–244.

Barretina, J., Caponigro, G., Stransky, N., Venkatesan, K., Margolin, A.A., Kim, S., Wilson, C.J., Lehar, J., Kryukov, G.V., Sonkin, D., et al. (2012). The Cancer Cell Line Encyclopedia enables predictive modelling of anticancer drug sensitivity. Nature *483*, 603–607.

Bhowmick, P., Mohammed, Y., and Borchers, C.H. (2018). MRMAssayDB: an integrated resource for validated targeted proteomics assays. Bioinformatics *34*, 3566–3571.

Boja, E.S., and Rodriguez, H. (2012). Mass spectrometry-based targeted quantitative proteomics: achieving sensitive and reproducible detection of proteins. Proteomics *12*, 1093–1110.

Bollag, G., Hirth, P., Tsai, J., Zhang, J., Ibrahim, P.N., Cho, H., Spevak, W., Zhang, C., Zhang, Y., Habets, G., et al. (2010). Clinical efficacy of a RAF inhibitor needs broad target blockade in BRAF-mutant melanoma. Nature *467*, 596–599. https://doi.org/10.1038/nature09454.

Burgess, M.W., Keshishian, H., Mani, D.R., Gillette, M.A., and Carr, S.A. (2014). Simplified and efficient quantification of low-abundance proteins at very high multiplex via targeted mass spectrometry. Mol. Cell Proteomics *13*, 1137–1149.

Carr, S.A., Abbatiello, S.E., Ackermann, B.L., Borchers, C., Domon, B., Deutsch, E.W., Grant, R.P., Hoofnagle, A.N., Huttenhain, R., Koomen, J.M., et al. (2014). Targeted peptide measurements in biology and medicine: best practices for mass spectrometry-based assay development using a fit-for-purpose approach. Mol. Cell Proteomics *13*, 907–917.

CCLE drug data.http://www.broadinstitute.org/ccle/.

Cerami, E., Gao, J., Dogrusoz, U., Gross, B.E., Sumer, S.O., Aksoy, B.A., Jacobsen, A., Byrne, C.J., Heuer, M.L., Larsson, E., et al. (2012). The cBio cancer genomics portal: an open platform for exploring multidimensional cancer genomics data. Cancer Discov. *2*, 401–404.

Chace, D.H., and Kalas, T.A. (2005). A biochemical perspective on the use of tandem mass spectrometry for newborn screening and clinical testing. Clin. Biochem. *38*, 296–309.

Chen, Y., Gruidl, M., Remily-Wood, E., Liu, R.Z., Eschrich, S., Lloyd, M., Nasir, A., Bui, M.M., Huang, E., Shibata, D., et al. (2010). Quantification of beta-catenin signaling components in colon cancer cell lines, tissue sections, and microdissected tumor cells using reaction monitoring mass spectrometry. J. Proteome Res. *9*, 4215–4227.

Corcoran, R.B., Ebi, H., Turke, A.B., Coffee, E.M., Nishino, M., Cogdill, A.P., Brown, R.D., Della Pelle, P., Dias-Santagata, D., Hung, K.E., et al. (2012). EGFR-mediated re-activation of MAPK signaling contributes to insensitivity of BRAF mutant colorectal cancers to RAF inhibition with vemurafenib. Cancer Discov. *2*, 227–235.

Cox, A.D., and Der, C.J. (2010). The raf inhibitor paradox: unexpected consequences of targeted drugs. Cancer Cell *17*, 221–223.

Cox, A.D., and Der, C.J. (2012). The RAF inhibitor paradox revisited. Cancer Cell *21*, 147–149.

Davies, H., Bignell, G.R., Cox, C., Stephens, P., Edkins, S., Clegg, S., Teague, J., Woffendin, H., Garnett, M.J., Bottomley, W., et al. (2002). Mutations of the BRAF gene in human cancer. Nature *417*, 949–954. https://doi.org/10.1038/nature00766.

Diao, L., and Chen, Y.G. (2007). PTEN, a general negative regulator of cyclin D expression. Cell Res *17*, 291–292.

Downward, J. (2003). Targeting RAS signalling pathways in cancer therapy. Nat. Rev. Cancer *3*, 11–22.

Eroglu, Z., Chen, Y.A., Gibney, G.T., Weber, J.S., Kudchadkar, R.R., Khushalani, N.I., Markowitz, J., Brohl, A.S., Tetteh, L.F., Ramadan, H., et al. (2018). Combined BRAF and HSP90 inhibition in patients with unresectable BRAF (V600E)-mutant melanoma. Clin. Cancer Res. *24*, 5516–5524.

Espona-Fiedler, M., Soto-Cerrato, V., Hosseini, A., Lizcano, J.M., Guallar, V., Quesada, R., Gao, T., and Perez-Tomas, R. (2012). Identification of dual mTORC1 and mTORC2 inhibitors in melanoma cells: prodigiosin vs. obatoclax. Biochem. Pharmacol. *83*, 489–496.

Fang, D., Hawke, D., Zheng, Y., Xia, Y., Meisenhelder, J., Nika, H., Mills, G.B., Kobayashi, R., Hunter, T., and Lu, Z. (2007). Phosphorylation of beta-catenin by AKT promotes beta-catenin transcriptional activity. J. Biol. Chem. *282*, 11221–11229.

Flaherty, K.T., Puzanov, I., Kim, K.B., Ribas, A., McArthur, G.A., Sosman, J.A., O'Dwyer, P.J., Lee, R.J., Grippo, J.F., Nolop, K., et al. (2010). Inhibition of Mutated, Activated BRAF in Metastatic Melanoma. The Journal of New England Medicine *363*, 809–819. https://doi.org/10.1056/NEJMoa1002011.

Gerber, S.A., Rush, J., Stemman, O., Kirschner, M.W., and Gygi, S.P. (2003). Absolute quantification of proteins and phosphoproteins from cell lysates by tandem MS. Proc. Natl. Acad. Sci. U S A. *100*, 6940–6945.

Gillette, M.A., and Carr, S.A. (2013). Quantitative analysis of peptides and proteins in biomedicine by targeted mass spectrometry. Nat. Methods *10*, 28–34.

Gopal, Y.N., Deng, W., Woodman, S.E., Komurov, K., Ram, P., Smith, P.D., and Davies, M.A. (2010). Basal and treatment-induced activation of AKT mediates resistance to cell death by AZD6244 (ARRY-142886) in Braf-mutant human cutaneous melanoma cells. Cancer Res. *70*, 8736–8747.

Gown, A.M. (2016). Diagnostic immunohistochemistry: what can go wrong and how to prevent it. Arch. Pathol. Lab Med. *140*, 893–898.

Gross, S., Rahal, R., Stransky, N., Lengauer, C., and Hoeflich, K.P. (2015). Targeting cancer with kinase inhibitors. J. Clin. Invest *125*, 1780–1789.

Herr, R., Halbach, S., Heizmann, M., Busch, H., Boerries, M., and Brummer, T. (2018). BRAF inhibition upregulates a variety of receptor tyrosine kinases and their downstream effector Gab2 in colorectal cancer cell lines. Oncogene *37*, 1576–1593.

Holderfield, M., Nagel, T.E., and Stuart, D.D. (2014). Mechanism and consequences of RAF kinase activation by small-molecule inhibitors. Br. J. Cancer *111*, 640–645.

Homsi, J., Cubitt, C.L., Zhang, S., Munster, P.N., Yu, H., Sullivan, D.M., Jove, R., Messina, J.L., and Daud, A.I. (2009). Src activation in melanoma and Src inhibitors as therapeutic agents in melanoma. Melanoma Res. *19*, 167–175.

Hornbeck, P.V., Kornhauser, J.M., Tkachev, S., Zhang, B., Skrzypek, E., Murray, B., Latham, V., and Sullivan, M. (2012). PhosphoSitePlus: a comprehensive resource for investigating the structure and function of experimentally determined post-translational modifications in man and mouse. Nucleic Acids Res. *40*, D261–D270.

Hornbeck, P.V., Kornhauser, J.M., Latham, V., Murray, B., Nandhikonda, V., Nord, A., Skrzypek, E., Wheeler, T., Zhang, B., and Gnad, F. (2019). 15 years of PhosphoSitePlus(R): integrating post-translationally modified sites, disease variants and isoforms. Nucleic Acids Res. *47*, D433–D441.

Huttenhain, R., Soste, M., Selevsek, N., Rost, H., Sethi, A., Carapito, C., Farrah, T., Deutsch, E.W., Kusebauch, U., Moritz, R.L., et al. (2012). Reproducible quantification of cancer-associated proteins in body fluids using targeted proteomics. Sci. Transl Med. *4*, 142ra194.

Ippoliti, P.J., Kuhn, E., Mani, D.R., Fagbami, L., Keshishian, H., Burgess, M.W., Jaffe, J.D., and Carr, S.A. (2016). Automated microchromatography enables multiplexing of immunoaffinity enrichment of peptides to greater than 150 for targeted MS-based assays. Anal Chem. *88*, 7548–7555.

Janes, K.A. (2015). An analysis of critical factors for quantitative immunoblotting. Sci. Signal *8*, rs2.

Jones, G.N., Rooney, C., Griffin, N., Roudier, M., Young, L.A., Garcia-Trinidad, A., Hughes, G.D., Whiteaker, J.R., Wilson, Z., Odedra, R., et al. (2018). pRAD50: a novel and clinically applicable pharmacodynamic biomarker of both ATM and ATR inhibition identified using mass spectrometry and immunohistochemistry. Br. J. Cancer *119*, 1233–1243.

Kennedy, J.J., Abbatiello, S.E., Kim, K., Yan, P., Whiteaker, J.R., Lin, C., Kim, J.S., Zhang, Y., Wang, X., Ivey, R.G., et al. (2014). Demonstrating the feasibility of large-scale development of standardized assays to quantify human proteins. Nat. Methods *11*, 149–155.

Kennedy, J.J., Yan, P., Zhao, L., Ivey, R.G., Voytovich, U.J., Moore, H.D., Lin, C., Pogosova-Agadjanyan, E.L., Stirewalt, D.L., Reding, K.W., et al. (2016). Immobilized metal affinity chromatography coupled to multiple reaction monitoring enables reproducible quantification of phospho-signaling. Mol. Cell Proteomics *15*, 726–739.

Khan, I., Rhett, J.M., and O'Bryan, J.P. (2020). Therapeutic targeting of RAS: new hope for drugging the "undruggable". Biochim. Biophys. Acta Mol. Cell Res *1867*, 118570.

Kuhn, E., Whiteaker, J.R., Mani, D.R., Jackson, A.M., Zhao, L., Pope, M.E., Smith, D., Rivera, K.D., Anderson, N.L., Skates, S.J., et al. (2012). Interlaboratory evaluation of automated, multiplexed peptide immunoaffinity enrichment coupled to multiple reaction monitoring mass spectrometry for quantifying proteins in plasma. Mol. Cell Proteomics *11*. https://doi.org/10.1074/mcp.M111.013854.

Kumar, M., Joseph, S.R., Augsburg, M., Bogdanova, A., Drechsel, D., Vastenhouw, N.L., Buchholz, F., Gentzel, M., and Shevchenko, A. (2018). MS Western, a method of multiplexed absolute protein quantification is a practical alternative to western blotting. Mol. Cell Proteomics *17*, 384–396.

Kusebauch, U., Campbell, D.S., Deutsch, E.W., Chu, C.S., Spicer, D.A., Brusniak, M.Y., Slagel, J., Sun, Z., Stevens, J., Grimes, B., et al. (2016). Human SRMAtlas: a resource of targeted assays to quantify the complete human proteome. Cell *166*, 766–778.

Lange, V., Picotti, P., Domon, B., and Aebersold, R. (2008). Selected reaction monitoring for quantitative proteomics: a tutorial. Mol. Syst. Biol. *4*, 222.

Lee, J.T., Li, L., Brafford, P.A., van den Eijnden, M., Halloran, M.B., Sproesser, K., Haass, N.K., Smalley, K.S., Tsai, J., Bollag, G., et al. (2010). PLX4032, a potent inhibitor of the B-Raf V600E oncogene, selectively inhibits V600E-positive melanomas. Pigment Cell Melanoma Res *23*, 820–827.

Lee, N., Lee, J.W., Kang, G.Y., Park, S.H., and Kim, K.P. (2019). Quantification of the dynamic phosphorylation process of ERK using stable isotope dilution selective reaction monitoring mass spectrometry. Proteomics *19*, e1900086.

Lito, P., Pratilas, C.A., Joseph, E.W., Tadi, M., Halilovic, E., Zubrowski, M., Huang, A., Wong, W.L., Callahan, M.K., Merghoub, T., et al. (2012). Relief of profound feedback inhibition of mitogenic signaling by RAF inhibitors attenuates their activity in BRAFV600E melanomas. Cancer Cell *22*, 668–682.

MacLean, B., Tomazela, D.M., Shulman, N., Chambers, M., Finney, G.L., Frewen, B., Kern, R., Tabb, D.L., Liebler, D.C., and MacCoss, M.J. (2010). Skyline: an open source document editor for creating and analyzing targeted proteomics experiments. Bioinformatics *26*, 966–968.

Paraiso, K.H., Xiang, Y., Rebecca, V.W., Abel, E.V., Chen, Y.A., Munko, A.C., Wood, E., Fedorenko, I.V., Sondak, V.K., Anderson, A.R., et al. (2011). PTEN loss confers BRAF inhibitor resistance to melanoma cells through the suppression of BIM expression. Cancer Res. *71*, 2750–2760.

Picotti, P., Bodenmiller, B., and Aebersold, R. (2013). Proteomics meets the scientific method. Nat. Methods *10*, 24–27.

Poulikakos, P.I., Zhang, C., Bollag, G., Shokat, K.M., and Rosen, N. (2010). RAF inhibitors transactivate RAF dimers and ERK signalling in cells with wild-type BRAF. Nature *464*, 427–430.

Prahallad, A., Sun, C., Huang, S., Di Nicolantonio, F., Salazar, R., Zecchin, D., Beijersbergen, R.L., Bardelli, A., and Bernards, R. (2012). Unresponsiveness of colon cancer to BRAF(V600E) inhibition through feedback activation of EGFR. Nature *483*, 100–103.

Rebecca, V.W., Wood, E., Fedorenko, I.V., Paraiso, K.H., Haarberg, H.E., Chen, Y., Xiang, Y., Sarnaik, A., Gibney, G.T., Sondak, V.K., et al. (2014). Evaluating melanoma drug response and therapeutic escape with quantitative proteomics. Mol. Cell Proteomics *13*, 1844–1854.

Remily-Wood, E.R., Liu, R.Z., Xiang, Y., Chen, Y., Thomas, C.E., Rajyaguru, N., Kaufman, L.M., Ochoa, J.E., Hazlehurst, L., Pinilla-Ibarz, J., et al. (2011). A database of reaction monitoring mass spectrometry assays for elucidating therapeutic response in cancer. Proteomics Clin. Appl. *5*, 383–396.

Remily-Wood, E.R., Benson, K., Baz, R.C., Chen, Y.A., Hussein, M., Hartley-Brown, M.A., Sprung, R.W., Perez, B., Liu, R.Z., Yoder, S.J., et al. (2014). Quantification of peptides from immunoglobulin constant and variable regions by LC-MRM MS for assessment of multiple myeloma patients. Proteomics Clin. Appl. *8*, 783–795.

Ritt, D.A., Monson, D.M., Specht, S.I., and Morrison, D.K. (2010). Impact of feedback phosphorylation and Raf heterodimerization on normal and mutant B-Raf signaling. Mol. Cell Biol *30*, 806–819.

Roberts, P.J., and Der, C.J. (2007). Targeting the Raf-MEK-ERK mitogen-activated protein kinase cascade for the treatment of cancer. Oncogene *26*, 3291–3310.

Saper, C.B. (2009). A guide to the perplexed on the specificity of antibodies. J. Histochem. Cytochem. *57*, 1–5.

Sarbassov, D.D., Guertin, D.A., Ali, S.M., and Sabatini, D.M. (2005). Phosphorylation and regulation of Akt/PKB by the rictor-mTOR complex. Science *307*, 1098–1101.

Schoenherr, R.M., Zhao, L., Ivey, R.G., Voytovich, U.J., Kennedy, J., Yan, P., Lin, C., Whiteaker, J.R., and Paulovich, A.G. (2016). Commercially available antibodies can be applied in quantitative multiplexed peptide immunoaffinity enrichment targeted mass spectrometry assays. Proteomics *16*, 2141–2145.

Schoenherr, R.M., Huang, D., Voytovich, U.J., Ivey, R.G., Kennedy, J.J., Saul, R.G., Colantonio, S., Roberts, R.R., Knotts, J.G., Kaczmarczyk, J.A., et al. (2019). A dataset describing a suite of novel antibody reagents for the RAS signaling network. Sci. Data *6*, 160.

Sharma, V., Eckels, J., Taylor, G.K., Shulman, N.J., Stergachis, A.B., Joyner, S.A., Yan, P., Whiteaker, J.R., Halusa, G.N., Schilling, B., et al. (2014). Panorama: a targeted proteomics knowledge base. J. Proteome Res. *13*, 4205–4210.

Sperling, A.S., Burgess, M., Keshishian, H., Gasser, J.A., Bhatt, S., Jan, M., Slabicki, M., Sellar, R.S., Fink, E.C., Miller, P.G., et al. (2019). Patterns of substrate affinity, competition, and degradation kinetics underlie biological activity of thalidomide analogs. Blood *134*, 160–170.

Tsai, J., Lee, J.T., Wang, W., Zhang, J., Cho, H., Mamo, S., Bremer, R., Gilette, S., Kong, J., Haass, N.K., et al. (2008). Discovery of a selective inhibitor of oncogenic B-Raf kinase with potent antimelanoma activity. Proc Natl Acad Sci U S A *105*, 3041–3046. https://doi.org/10.1073/pnas.0711741105.

Tse, A., and Verkhivker, G.M. (2016). Exploring molecular mechanisms of paradoxical activation in the BRAF kinase dimers: atomistic simulations of conformational dynamics and modeling of allosteric communication networks and signaling pathways. PLoS One *11*, e0166583.

Walker, R.A. (2006). Quantification of immunohistochemistry—issues concerning methods, utility and semiquantitative assessment I. Histopathology *49*, 406–410.

Wang, P., Whiteaker, J.R., and Paulovich, A.G. (2009). The evolving role of mass spectrometry in cancer biomarker discovery. Cancer Biol. Ther. *8*, 1083–1094.

Want, E.J., Cravatt, B.F., and Siuzdak, G. (2005). The expanding role of mass spectrometry in metabolite profiling and characterization. Chembiochem *6*, 1941–1951.

Whiteaker, J.R., Zhao, L., Abbatiello, S.E., Burgess, M., Kuhn, E., Lin, C., Pope, M.E., Razavi, M., Anderson, N.L., Pearson, T.W., et al. (2011). Evaluation of large scale quantitative proteomic assay development using peptide affinity-based mass spectrometry. Mol. Cell Proteomics *10*. https://doi.org/10.1074/mcp.M110.005645.

Whiteaker, J.R., Halusa, G.N., Hoofnagle, A.N., Sharma, V., MacLean, B., Yan, P., Wrobel, J.A., Kennedy, J., Mani, D.R., Zimmerman, L.J., et al. (2014). CPTAC assay portal: a repository of targeted proteomic assays. Nat. Methods *11*, 703–704.

Whiteaker, J.R., Halusa, G.N., Hoofnagle, A.N., Sharma, V., MacLean, B., Yan, P., Wrobel, J.A., Kennedy, J., Mani, D.R., Zimmerman, L.J., et al. (2016). Using the CPTAC assay portal to identify and implement highly characterized targeted proteomics assays. Methods Mol. Biol. *1410*, 223–236.

Whiteaker, J.R., Zhao, L., Saul, R., Kaczmarczyk, J.A., Schoenherr, R.M., Moore, H.D., Jones-Weinert, C., Ivey, R.G., Lin, C., Hiltke, T., et al. (2018). A multiplexed mass spectrometry-based assay for robust quantification of phosphosignaling in response to DNA damage. Radiat. Res. *189*, 505–518.

Young, A., Lyons, J., Miller, A.L., Phan, V.T., Alarcon, I.R., and McCormick, F. (2009). Ras signaling and therapies. Adv. Cancer Res. *102*, 1–17.

CellPress
OPEN ACCESS

STAR★METHODS

KEY RESOURCES TABLE

REAGENT or RESOURCE	SOURCE	IDENTIFIER
Antibodies		
Monoclonal anti-AKT1	antibodies.cancer.gov	RRID: AB_2722014
Monoclonal anti-AKT1	antibodies.cancer.gov	RRID: AB_2868548
Monoclonal anti-AKT1	antibodies.cancer.gov	RRID: AB_2722012
Monoclonal anti-AKT1	antibodies.cancer.gov	RRID: AB_2722013
Monoclonal anti-AKT1	antibodies.cancer.gov	RRID: AB_2868548
Monoclonal anti-AKT1	antibodies.cancer.gov	RRID: AB_2827858
Monoclonal anti-AKT2	antibodies.cancer.gov	RRID: AB_2868549
Monoclonal anti-AKT2	antibodies.cancer.gov	RRID: AB_2868549
Monoclonal anti-AKT2	antibodies.cancer.gov	RRID: AB_2722017
Monoclonal anti-AKT2	antibodies.cancer.gov	RRID: AB_2722015
Monoclonal anti-AKT2	antibodies.cancer.gov	RRID: AB_2722015
Monoclonal anti-AKT3	antibodies.cancer.gov	RRID: AB_2814780
Monoclonal anti-AKT3	antibodies.cancer.gov	RRID: AB_2814778
Monoclonal anti-AKT3	antibodies.cancer.gov	RRID: AB_2722019
Monoclonal anti-AKT3	antibodies.cancer.gov	RRID: AB_2722019
Monoclonal anti-AKT3	antibodies.cancer.gov	RRID: AB_2820256
Monoclonal anti-AKT3	antibodies.cancer.gov	RRID: AB_2820256
Monoclonal anti-CDH1	antibodies.cancer.gov	RRID: AB_2722038
Monoclonal anti-CDH1	antibodies.cancer.gov	RRID: AB_2722039
Monoclonal anti-CDH2	antibodies.cancer.gov	RRID: AB_2722042
Monoclonal anti-CDH2	antibodies.cancer.gov	RRID: AB_2722044
Monoclonal anti-PTEN	antibodies.cancer.gov	RRID: AB_2617320
Monoclonal anti-PTEN	antibodies.cancer.gov	RRID: AB_2722096
Monoclonal anti-PTEN	antibodies.cancer.gov	RRID: AB_2722095
Monoclonal anti-ARAF	antibodies.cancer.gov	RRID: AB_2722023
Monoclonal anti-ARAF	antibodies.cancer.gov	RRID: AB_2827857
Monoclonal anti-ARAF	antibodies.cancer.gov	RRID: AB_2722020
Monoclonal anti-ARAF	antibodies.cancer.gov	RRID: AB_2722021
Monoclonal anti-ARAF	antibodies.cancer.gov	RRID: AB_2722022
Monoclonal anti-ARAF	antibodies.cancer.gov	RRID: AB_2722023
Monoclonal anti-ARAF	antibodies.cancer.gov	RRID: AB_2827857
Monoclonal anti-BRAF	antibodies.cancer.gov	RRID: AB_2722029
Monoclonal anti-BRAF	antibodies.cancer.gov	RRID: AB_2722024
Monoclonal anti-BRAF	antibodies.cancer.gov	RRID: AB_2722027
Monoclonal anti-BRAF	antibodies.cancer.gov	RRID: AB_2722027
Monoclonal anti-BRAF	antibodies.cancer.gov	RRID: AB_2827860
Monoclonal anti-BRAF	antibodies.cancer.gov	RRID: AB_2722027
Monoclonal anti-BRAF	antibodies.cancer.gov	RRID: AB_2722027
Monoclonal anti-RAF1	antibodies.cancer.gov	RRID: AB_2868553
Monoclonal anti-RAF1	antibodies.cancer.gov	RRID: AB_2868552
Monoclonal anti-RAF1	antibodies.cancer.gov	RRID: AB_2868554
Monoclonal anti-RAF1	antibodies.cancer.gov	RRID: AB_2868551

(*Continued on next page*)

Continued

REAGENT or RESOURCE	SOURCE	IDENTIFIER
Monoclonal anti-RAF1	antibodies.cancer.gov	RRID: AB_2827856
Monoclonal anti-MAP2K1	antibodies.cancer.gov	RRID: AB_2722079
Monoclonal anti-MTOR	antibodies.cancer.gov	RRID: AB_2722092
Monoclonal anti-MTOR	antibodies.cancer.gov	RRID: AB_2722091
Monoclonal anti-MTOR	antibodies.cancer.gov	RRID: AB_2722087
Monoclonal anti-MTOR	antibodies.cancer.gov	RRID: AB_2722090
Monoclonal anti-MTOR	antibodies.cancer.gov	RRID: AB_2722085
Monoclonal anti-MTOR	antibodies.cancer.gov	RRID: AB_2722085
Monoclonal anti-MTOR	antibodies.cancer.gov	RRID: AB_2722086
Monoclonal anti-MTOR	antibodies.cancer.gov	RRID: AB_2722086
Monoclonal anti-MTOR	antibodies.cancer.gov	RRID: AB_2722088
Monoclonal anti-MTOR	antibodies.cancer.gov	RRID: AB_2722085
Monoclonal anti-MTOR	antibodies.cancer.gov	RRID: AB_2722085
Monoclonal anti-MTOR	antibodies.cancer.gov	RRID: AB_2820270
Monoclonal anti-MTOR	antibodies.cancer.gov	RRID: AB_2820270
Monoclonal anti-GSK3B	antibodies.cancer.gov	RRID: AB_2722062
Monoclonal anti-GSK3B	antibodies.cancer.gov	RRID: AB_2722063
Monoclonal anti-GSK3B	antibodies.cancer.gov	RRID: AB_2722064
Monoclonal anti-GSK3B	antibodies.cancer.gov	RRID: AB_2722068
Monoclonal anti-GSK3B	antibodies.cancer.gov	RRID: AB_2827872
Monoclonal anti-MAPK1	antibodies.cancer.gov	RRID: AB_2827852
Monoclonal anti-MAPK1	antibodies.cancer.gov	RRID: AB_2827852
Monoclonal anti-MAPK1	antibodies.cancer.gov	RRID: AB_2827852
Monoclonal anti-MAPK1	antibodies.cancer.gov	RRID: AB_2827852
Monoclonal anti-MAPK3	antibodies.cancer.gov	RRID: AB_2722081
Monoclonal anti-MAPK1	antibodies.cancer.gov	RRID: AB_2827852
Monoclonal anti-MAPK1	antibodies.cancer.gov	RRID: AB_2827852
Monoclonal anti-MAPK1	antibodies.cancer.gov	RRID: AB_2827852
Monoclonal anti-MAPK1	antibodies.cancer.gov	RRID: AB_2827852
Monoclonal anti-FOS	antibodies.cancer.gov	RRID: AB_2722060
Monoclonal anti-FOS	antibodies.cancer.gov	RRID: AB_2722061
Monoclonal anti-FOS	antibodies.cancer.gov	RRID: AB_2722059
Monoclonal anti-EGFR	antibodies.cancer.gov	RRID: AB_2722047
Monoclonal anti-EGFR	antibodies.cancer.gov	RRID: AB_2722050
Monoclonal anti-EGFR	antibodies.cancer.gov	RRID: AB_2722051
Monoclonal anti-EGFR	antibodies.cancer.gov	RRID: AB_2722048
Monoclonal anti-EGFR	antibodies.cancer.gov	RRID: AB_2827844
Monoclonal anti-EGFR	antibodies.cancer.gov	RRID: AB_2827844
Monoclonal anti-EGFR	antibodies.cancer.gov	RRID: AB_2827846
Monoclonal anti-EGFR	antibodies.cancer.gov	RRID: AB_2827847
Monoclonal anti-EGFR	antibodies.cancer.gov	RRID: AB_2827849
Monoclonal anti-ERBB2	antibodies.cancer.gov	RRID: AB_2722052
Monoclonal anti-ERBB2	antibodies.cancer.gov	RRID: AB_2722053
Monoclonal anti-ERBB2	antibodies.cancer.gov	RRID: AB_2827851
Monoclonal anti-ERBB2	antibodies.cancer.gov	RRID: AB_2722053
Monoclonal anti-ERBB3	antibodies.cancer.gov	RRID: AB_2722054
Monoclonal anti-ERBB3	antibodies.cancer.gov	RRID: AB_2722055
Monoclonal anti-ERBB3	antibodies.cancer.gov	RRID: AB_2722057

(*Continued on next page*)

Continued

REAGENT or RESOURCE	SOURCE	IDENTIFIER
Monoclonal anti-ERBB3	antibodies.cancer.gov	RRID: AB_2722056
Monoclonal anti-CCND1	antibodies.cancer.gov	RRID: AB_2722036
Monoclonal anti-CCND1	antibodies.cancer.gov	RRID: AB_2868550
Monoclonal anti-CCND1	antibodies.cancer.gov	RRID: AB_2722033
Monoclonal anti-CCND1	antibodies.cancer.gov	RRID: AB_2722031
Monoclonal anti-CCND1	antibodies.cancer.gov	RRID: AB_2722032
Monoclonal anti-RPTOR	antibodies.cancer.gov	RRID: AB_2722104
Monoclonal anti-RPTOR	antibodies.cancer.gov	RRID: AB_2722103
anti-Pan AKT	Cell Signaling	cat#2920; RRID: AB_1147620
anti-P-AKT S473	Cell Signaling	cat#4060; RRID: AB_2315049
anti-Pan MEK	Cell Signaling	cat#4694; RRID: AB_10695868
anti-P-MEK S217/221	Cell Signaling	cat#9154; RRID: AB_2138017
anti-Erk 1/2	Cell Signaling	cat#4696; RRID: AB_390780
anti-P-ERK 1/2	Cell Signaling	cat#9101; RRID: AB_331646
anti-EGFR	Cell Signaling	cat#2646; RRID: AB_2230881
anti-P-EGFR Y1068	Cell Signaling	cat#3777; RRID: AB_2096270
anti-PTEN	Cell Signaling	cat#9559; RRID: AB_390810
anti-AKT3	Cell Signaling	cat#4059; RRID: AB_2225351
anti-CCND1	Cell Signaling	cat#2978; RRID: AB_10699151
anti-ERBB2	Cell Signaling	cat#4290; RRID: AB_10557104
anti-P-CTNNB1 S552	Cell Signaling	cat#5651; RRID: AB_10831053
anti-N-Cadherin	Cell Signaling	cat#13116; RRID: AB_2687616
anti-P-GSK3B S9	Cell Signaling	cat#5585; RRID: AB_10706782
anti-E-Cadherin	Cell Signaling	cat#3195; RRID: AB_2291471
anti-CRAF	Cell Signaling	cat#53745; RRID: AB_2799444
anti-P-PRAS40 T246	Cell Signaling	cat#13175; RRID: AB_2798140
anti-RSK1	Cell Signaling	cat#9333; RRID: AB_2181177
anti-Vinculin	Cell Signaling	cat#13901; RRID: AB_2728768
anti-Erbb3	Cell Signaling	cat#12708; RRID: AB_2721919
anti-stat3	Cell Signaling	cat#9139; RRID: AB_331757
anti-eIF2alpha	Cell Signaling	cat#2103; RRID: AB_836874
anti-B-Raf	Cell Signaling	cat#14814; RRID: AB_2750887
anti-C-Raf	Cell Signaling	cat#53745; RRID: AB_2799444
anti-A-Raf	Cell Signaling	cat#4432; RRID: AB_330813
anti-P-p90RSK T359/s363	Cell Signaling	cat#9344; RRID: AB_331650
anti-P-c-Raf S338	Cell Signaling	cat#9427; RRID: AB_2067317
Chemicals, peptides, and recombinant proteins		
Stable Isotope Labeled Synthetic Peptides	New England Peptide	Custom by sequence
Critical commercial assays		
CellTiter-Glo® Luminescent Cell Viability	Promega	G7570
Deposited data		
Raw Data	PanoramaWeb	https://panoramaweb.org/NmDXGW.url
Experimental models: cell lines		
HCT116	ATCC	CCL-247
HT29	ATCC	HTB-38
A375	ATCC	CRL-1619
SKMEL2	ATCC	HTB-68

(*Continued on next page*)

Continued

REAGENT or RESOURCE	SOURCE	IDENTIFIER
MRM assays		
AKT1_FFAGIVWQHVYEK_direct	assays.cancer.gov	non-CPTAC-5528
AKT1_FYGAEIVSALDYLHSEK_direct	assays.cancer.gov	non-CPTAC-5328
AKT1_RPHFPQFSYSASGTA_direct	assays.cancer.gov	non-CPTAC-5332
AKT1_SLLSGLLK_direct	assays.cancer.gov	non-CPTAC-5527
AKT2_EGISDGATMK_direct	assays.cancer.gov	non-CPTAC-5335
AKT2_FYGAEIVSALEYLHSR_direct	assays.cancer.gov	non-CPTAC-5334
AKT2_LLPPFKPQVTSEVDTR_direct	assays.cancer.gov	non-CPTAC-5529
AKT2_SLLAGLLK_direct	assays.cancer.gov	non-CPTAC-5336
AKT2_THFPQFSYSASIRE_direct	assays.cancer.gov	non-CPTAC-5338
AKT2_THFPQFSYSASIR_direct	assays.cancer.gov	non-CPTAC-5339
AKT3_DEVAHTLTESR_direct	assays.cancer.gov	non-CPTAC-5530
AKT3_EGITDAATMK_direct	assays.cancer.gov	non-CPTAC-5531
AKT3_FYGAEIVSALDYLHSGK_direct	assays.cancer.gov	non-CPTAC-5342
AKT3_RPHFPQFSYSASGR_direct	assays.cancer.gov	non-CPTAC-5344
AKT3_RPHFPQFSYSASGRE_direct	assays.cancer.gov	non-CPTAC-5345
AKT3_TDGSFIGYK_direct	assays.cancer.gov	non-CPTAC-5340
CDH1_GLDARPEVTR_direct	assays.cancer.gov	non-CPTAC-5542
CDH1_GQVPENEANVVITTLK_direct	assays.cancer.gov	non-CPTAC-5541
CDH1_NDVAPTLMSVPR_direct	assays.cancer.gov	non-CPTAC-5370
CDH1_NTGVISVVTTGLDR_direct	assays.cancer.gov	non-CPTAC-5367
CDH1_TAYFSLDTR_direct	assays.cancer.gov	non-CPTAC-5366
CDH2_GPFPQELVR_direct	assays.cancer.gov	non-CPTAC-5371
CDH2_IDPVNGQITTIAVLDR_direct	assays.cancer.gov	non-CPTAC-5373
CDH2_LNGDFAQLNLK_direct	assays.cancer.gov	non-CPTAC-5374
CDH2_LSDPANWLK_direct	assays.cancer.gov	non-CPTAC-5543
CDH2_SAAPHPGDIGDFINEGLK_direct	assays.cancer.gov	non-CPTAC-5544
CTNNB1_RTSMGGTQQQFVEGVR_direct	assays.cancer.gov	non-CPTAC-3265
PTEN_AQEALDFYGEVR_direct	assays.cancer.gov	non-CPTAC-5566
PTEN_GVTIPSQR_direct	assays.cancer.gov	non-CPTAC-5567
PTEN_IYSSNSGPTR_direct	assays.cancer.gov	non-CPTAC-5430
PTEN_NHLDYRPVALLFHK_direct	assays.cancer.gov	non-CPTAC-5429
ARAF_DSGYYWEVPPSEVQLLK_direct	assays.cancer.gov	non-CPTAC-5348
ARAF_NLGYRDSGYYWEVPPSEVQLLK_direct	assays.cancer.gov	non-CPTAC-5347
ARAF_IGTGSFGTVFR_direct	assays.cancer.gov	non-CPTAC-5533
ARAF_VSQPTAEQAQAFK_direct	assays.cancer.gov	non-CPTAC-5350
BRAF_GDGGSTTGLSATPPASLPGSLTNVK_direct	assays.cancer.gov	non-CPTAC-5353
BRAF_RDSSDDWEIPDGQITVGQR_direct	assays.cancer.gov	non-CPTAC-5354
BRAF_DSSDDWEIPDGQITVGQR_direct	assays.cancer.gov	non-CPTAC-5355
BRAF_SNNIFLHEDLTVK_direct	assays.cancer.gov	non-CPTAC-5356
RAF1_DSSYYWEIEASEVMLSTR_direct	assays.cancer.gov	non-CPTAC-5433
RAF1_GYASPDLSK_direct	assays.cancer.gov	non-CPTAC-5570
RAF1_STSTPNVHMVSTTLPVDSR_direct	assays.cancer.gov	non-CPTAC-5432
RAF1_VVDPTPEQFQAFR_direct	assays.cancer.gov	non-CPTAC-5569
MAP2K1_IPEQILGK_direct	assays.cancer.gov	non-CPTAC-5411
MAP2K1_ISELGAGNGGVVFK_direct	assays.cancer.gov	non-CPTAC-5557
MAP2K1_VSHKPSGLVMAR_direct	assays.cancer.gov	non-CPTAC-5410
MTOR_DLELAVPGTYDPNQPIIR_direct	assays.cancer.gov	non-CPTAC-5563
MTOR_IQSIAPSLQVITSK_direct	assays.cancer.gov	non-CPTAC-5421

(*Continued on next page*)

CellPress
OPEN ACCESS

Continued

REAGENT or RESOURCE	SOURCE	IDENTIFIER
MTOR_LFDAPEAPLPSR_direct	assays.cancer.gov	non-CPTAC-5561
MTOR_LTESLDFTDYASR_direct	assays.cancer.gov	non-CPTAC-5562
MTOR_TDSYSAGQSVEILDGVELGEPAHK_direct	assays.cancer.gov	non-CPTAC-5423
MTOR_TRTDSYSAGQSVEILDGVELGEPAHK_direct	assays.cancer.gov	non-CPTAC-5422
MTOR_TGTTVPESIHSFIGDGLVKPEALNK_direct	assays.cancer.gov	non-CPTAC-5424
MTOR_TGTTVPESIHSFIGDGLVKPEALNKK_direct	assays.cancer.gov	non-CPTAC-5425
MTOR_VLGLLGALDPYK_direct	assays.cancer.gov	non-CPTAC-5560
GSK3B_LLEYTPTAR_direct	assays.cancer.gov	non-CPTAC-5556
GSK3B_QTLPVIYVK_direct	assays.cancer.gov	non-CPTAC-5403
GSK3B_VIGNGSFGVVYQAK_direct	assays.cancer.gov	non-CPTAC-5554
MAPK3_ALDLLDR_direct	assays.cancer.gov	non-CPTAC-5559
MAPK3_GQPFDVGPR_direct	assays.cancer.gov	non-CPTAC-5412
MAPK3_IADPEHDHTGFLTEYVATR_direct	assays.cancer.gov	non-CPTAC-5414
MAPK3_NYLQSLPSK_direct	assays.cancer.gov	non-CPTAC-5415
FOS_APHPFGVPAPSAGAYSR_direct	assays.cancer.gov	non-CPTAC-5551
FOS_GSSSNEPSSDSLSSPTLLAL_direct	assays.cancer.gov	non-CPTAC-5553
FOS_LEFILAAHR_direct	assays.cancer.gov	non-CPTAC-5398
FOS_SALQTEIANLLK_direct	assays.cancer.gov	non-CPTAC-5397
FOS_TEPFDDFLFPASSR_direct	assays.cancer.gov	non-CPTAC-5552
EGFR_GSHQISLDNPDYQQDFFPK_direct	assays.cancer.gov	non-CPTAC-5381
EGFR_GSTAENAEYLR_direct	assays.cancer.gov	non-CPTAC-5382
EGFR_IPLENLQIIR_direct	assays.cancer.gov	non-CPTAC-5545
EGFR_NLQEILHGAVR_direct	assays.cancer.gov	non-CPTAC-5546
EGFR_YSSDPTGALTEDSIDDTFLPVPEYINQSVPK_direct	assays.cancer.gov	non-CPTAC-5380
ERBB2_ELVSEFSR_direct	assays.cancer.gov	non-CPTAC-5385
ERBB2_GIWIPDGENVK_direct	assays.cancer.gov	non-CPTAC-5547
ERBB2_GTPTAENPEYLGLDVPV_direct	assays.cancer.gov	non-CPTAC-5386
ERBB2_LLDIDETEYHADGGK_direct	assays.cancer.gov	non-CPTAC-5384
ERBB3_ANDALQVLGLLFSLAR_direct	assays.cancer.gov	non-CPTAC-5387
ERBB3_GDSAYHSQR_direct	assays.cancer.gov	non-CPTAC-5390
ERBB3_LTFQLEPNPHTK_direct	assays.cancer.gov	non-CPTAC-5548
ERBB3_SLEATDSAFDNPDYWHSR_direct	assays.cancer.gov	non-CPTAC-5550
ERBB3_YLERGESIEPLDPSEK_direct	assays.cancer.gov	non-CPTAC-5549
CCND1_AYPDANLLNDR_direct	assays.cancer.gov	non-CPTAC-5536
CCND1_FLSLEPVKK_direct	assays.cancer.gov	non-CPTAC-5538
CCND1_FLSLEPVK_direct	assays.cancer.gov	non-CPTAC-5360
RPTOR_ALETIGANLQK_direct	assays.cancer.gov	non-CPTAC-5441
RPTOR_SLIVAGLGDGSIR_direct	assays.cancer.gov	non-CPTAC-5445
RPTOR_VLDTSSLTQSAPASPTNK_direct	assays.cancer.gov	non-CPTAC-5444
RPTOR_VLNSIAYK_direct	assays.cancer.gov	non-CPTAC-5443
RASGRF1_LLYGEPPKSPR_direct	assays.cancer.gov	non-CPTAC-5438
RASGRF1_NSLDYAK_direct	assays.cancer.gov	non-CPTAC-5436
RASGRF1_SLELLFASGQNNK_direct	assays.cancer.gov	non-CPTAC-5437
EIF2A_SPDLAPTPAPQSTPR_direct	assays.cancer.gov	non-CPTAC-5377
FOXO3_AVSMDNSNK_direct	assays.cancer.gov	non-CPTAC-5392
FOXO3_AVSMDNSNKYTK_direct	assays.cancer.gov	non-CPTAC-5394
MAPK8_TAGTSFMMTPYVVTR_direct	assays.cancer.gov	non-CPTAC-5407
RPS6KA1_GFSFVATGLMEDDGKPR_direct	assays.cancer.gov	non-CPTAC-5446
AKT1S1_LNTSDFQK_direct	assays.cancer.gov	non-CPTAC-5333

(*Continued on next page*)

Continued

REAGENT or RESOURCE	SOURCE	IDENTIFIER
AKT1_RPHFPQFS[+80]YSASGTA_S473_IMAC	assays.cancer.gov	non-CPTAC-5720
AKT1_T[+80]FC[+57]GTPEYLAPEVLEDNDYGR_T308_IMAC	assays.cancer.gov	non-CPTAC-5719
AKT2_THFPQFS[+80]YSASIRE_S473_IMAC	assays.cancer.gov	non-CPTAC-5718
AKT2_THFPQFS[+80]YSASIR_S473_IMAC	assays.cancer.gov	non-CPTAC-5717
AKT3_RPHFPQFS[+80]YSASGR_S472_IMAC	assays.cancer.gov	non-CPTAC-5693
AKT3_RPHFPQFS[+80]YSASGRE_S472_IMAC	assays.cancer.gov	non-CPTAC-5692
CTNNB1_TS[+80]MGGTQQQFVEGVR_S552_IMAC	assays.cancer.gov	non-CPTAC-5715
CTNNB1_RTS[+80]MGGTQQQFVEGVR_S552_IMAC	assays.cancer.gov	non-CPTAC-5716
ARAF_DS[+80]GYYWEVPPSEVQLLK_S299_IMAC	assays.cancer.gov	non-CPTAC-5730
ARAF_NLGYRDS[+80]GYYWEVPPSEVQLLK_S299_IMAC	assays.cancer.gov	non-CPTAC-5731
BRAF_GDGGSTTGLSAT[+80]PPASLPGSLTNVK_T401_IMAC	assays.cancer.gov	non-CPTAC-5729
BRAF_DS[+80]SDDWEIPDGQITVGQR_S446_IMAC	assays.cancer.gov	non-CPTAC-5727
BRAF_RDS[+80]SDDWEIPDGQITVGQR_S446_IMAC	assays.cancer.gov	non-CPTAC-5728
RAF1_STS[+80]TPNVHMVSTTLPVDSR_S259_IMAC	assays.cancer.gov	non-CPTAC-5734
MAP2K2_LC[+57]DFGVSGQLIDS[+80] MANSFVGTR_S221_IMAC	assays.cancer.gov	non-CPTAC-5704
MTOR_TDS[+80]YSAGQSVEILDGVELGEPAHK_S2448_IMAC	assays.cancer.gov	non-CPTAC-5711
MTOR_TRTDS[+80]YSAGQSVEILDGVELGEPAHK_S2448_IMAC	assays.cancer.gov	non-CPTAC-5712
MTOR_TGTTVPESIHS[+80]FIGDGLVKPEALNK_S2481_IMAC	assays.cancer.gov	non-CPTAC-5709
MTOR_TGTTVPESIHS[+80]FIGDGLVKPEALNKK_S2481_IMAC	assays.cancer.gov	non-CPTAC-5710
GSK3B_TTS[+80]FAESC[+57]KPVQQPSAFGSMK_S9_IMAC	assays.cancer.gov	non-CPTAC-5705
MAPK1_VADPDHDHTGFLT[+80]EY[+80]VATR_T185/ Y187_IMAC	assays.cancer.gov	non-CPTAC-5723
MAPK1_VADPDHDHTGFLT[+80]EYVATR_T185_IMAC	assays.cancer.gov	non-CPTAC-5721
MAPK1_VADPDHDHTGFLTEY[+80]VATR_Y187_IMAC	assays.cancer.gov	non-CPTAC-5722
MAPK3_IADPEHDHTGFLT[+80]EY[+80]VATR_T202/Y204_IMAC	assays.cancer.gov	non-CPTAC-5726
MAPK3_IADPEHDHTGFLT[+80]EYVATR_T202_IMAC	assays.cancer.gov	non-CPTAC-5724
MAPK3_IADPEHDHTGFLTEY[+80]VATR_Y204_IMAC	assays.cancer.gov	non-CPTAC-5725
EGFR_Y[+80] SSDPTGALTEDSIDDTFLPVPEYINQSVPK_Y1045_IMAC	assays.cancer.gov	non-CPTAC-5738
EGFR_YSSDPTGALTEDSIDDTFLPVPEY[+80] INQSVPK_Y1068_IMAC	assays.cancer.gov	non-CPTAC-5735
EGFR_GSHQISLDNPDY[+80]QQDFFPK_Y1148_IMAC	assays.cancer.gov	non-CPTAC-5737
EGFR_GSTAENAEY[+80]LR_Y1173_IMAC	assays.cancer.gov	non-CPTAC-5736
ERBB2_GTPTAENPEY[+80]LGLDVPV_Y1248_IMAC	assays.cancer.gov	non-CPTAC-5732
ERBB2_LLDIDETEY[+80]HADGGK_Y877_IMAC	assays.cancer.gov	non-CPTAC-5733
EIF2A_SPDLAPTPAPQST[+80]PR_T518_IMAC	assays.cancer.gov	non-CPTAC-5694
EIF2A_SDKSPDLAPTPAPQST[+80]PR_T518_IMAC	assays.cancer.gov	non-CPTAC-5695
EIF2A_S[+80]PDLAPTPAPQSTPR_T506_IMAC	assays.cancer.gov	non-CPTAC-5696
EIF2A_SDKS[+80]PDLAPTPAPQSTPR_T506_IMAC	assays.cancer.gov	non-CPTAC-5697
FOXO1_AAS[+80]MDNNSK_S256_IMAC	assays.cancer.gov	non-CPTAC-5703
FOXO3_AVS[+80]MDNSNK_S253_IMAC	assays.cancer.gov	non-CPTAC-5740
FOXO3_AVS[+80]MDNSNKYTK_S253_IMAC	assays.cancer.gov	non-CPTAC-5739
MAPK8_TAGTSFMMT[+80]PY[+80]VVTR_T183/Y185_IMAC	assays.cancer.gov	non-CPTAC-5708
MAPK8_TAGTSFMMT[+80]PYVVTR_T183_IMAC	assays.cancer.gov	non-CPTAC-5706
MAPK8_TAGTSFMMTPY[+80]VVTR_Y185_IMAC	assays.cancer.gov	non-CPTAC-5707
MAPK14_HTDDEMT[+80]GY[+80]VATR_T180/Y182_IMAC	assays.cancer.gov	non-CPTAC-5699
MAPK14_HTDDEMT[+80]GYVATR_T180_IMAC	assays.cancer.gov	non-CPTAC-5701
MAPK14_HTDDEMTGY[+80]VATR_Y182_IMAC	assays.cancer.gov	non-CPTAC-5700
RPS6KA1_GFS[+80]FVATGLMEDDGKPR_S380_IMAC	assays.cancer.gov	non-CPTAC-5702

(*Continued on next page*)

Continued

REAGENT or RESOURCE	SOURCE	IDENTIFIER
AKT1S1_LNT[+80]SDFQK_T246_IMAC	assays.cancer.gov	non-CPTAC-5698
STAT3_FIC[+57]VTPTTC[+57]SNTIDLPMS[+80]PR_S727_IMAC	assays.cancer.gov	non-CPTAC-5713
STAT3_YC[+57]RPESQEHPEADPGSAAPY[+80]LK_Y705_IMAC	assays.cancer.gov	non-CPTAC-5714
AKT1_FFAGIVWQHVYEK_immuno	assays.cancer.gov	CPTAC-5758
AKT1_RPHFPQFSYSASGTA_immuno	assays.cancer.gov	CPTAC-5806
AKT1_SLLSGLLK_immuno	assays.cancer.gov	CPTAC-5759
AKT1_TFC[+57]GTPEYLAPEVLEDNDYGR_immuno	assays.cancer.gov	CPTAC-5808
AKT1_RPHFPQFS[+80]YSASGTA_S473_immuno	assays.cancer.gov	CPTAC-5805
AKT1_T[+80]FC[+57]GTPEYLAPEVLEDNDYGR_T308_immuno	assays.cancer.gov	CPTAC-5807
AKT2_THFPQFS[+80]YSASIRE_S473_immuno	assays.cancer.gov	CPTAC-5804
AKT2_THFPQFS[+80]YSASIR_S473_immuno	assays.cancer.gov	CPTAC-5802
AKT2_LLPPFKPQVTSEVDTR_immuno	assays.cancer.gov	CPTAC-5757
AKT2_THFPQFSYSASIRE_immuno	assays.cancer.gov	CPTAC-5803
AKT2_THFPQFSYSASIR_immuno	assays.cancer.gov	CPTAC-5801
AKT3_EGITDAATMK_immuno	assays.cancer.gov	CPTAC-5742
AKT3_RPHFPQFSYSASGR_immuno	assays.cancer.gov	CPTAC-5788
AKT3_RPHFPQFSYSASGRE_immuno	assays.cancer.gov	CPTAC-5786
AKT3_RPHFPQFS[+80]YSASGR_S472_immuno	assays.cancer.gov	CPTAC-5789
AKT3_RPHFPQFS[+80]YSASGRE_S472_immuno	assays.cancer.gov	CPTAC-5787
CDH1_GLDARPEVTR_immuno	assays.cancer.gov	CPTAC-5772
CDH1_GQVPENEANVVITTLK_immuno	assays.cancer.gov	CPTAC-5773
CDH2_LSDPANWLK_immuno	assays.cancer.gov	CPTAC-5770
CDH2_SAAPHPGDIGDFINEGLK_immuno	assays.cancer.gov	CPTAC-5769
PTEN_AQEALDFYGEVR_immuno	assays.cancer.gov	CPTAC-5747
PTEN_GVTIPSQR_immuno	assays.cancer.gov	CPTAC-5746
PTEN_IYNLC[+57]AER_immuno	assays.cancer.gov	CPTAC-5748
ARAF_DSGYYWEVPPSEVQLLK_immuno	assays.cancer.gov	CPTAC-5823
ARAF_NLGYRDSGYYWEVPPSEVQLLK_immuno	assays.cancer.gov	CPTAC-5825
ARAF_GLNQDC[+57]C[+57]VVYR_immuno	assays.cancer.gov	CPTAC-5776
ARAF_IGTGSFGTVFR_immuno	assays.cancer.gov	CPTAC-5775
ARAF_TQADELPAC[+57]LLSAAR_immuno	assays.cancer.gov	CPTAC-5774
ARAF_DS[+80]GYYWEVPPSEVQLLK_S299_immuno	assays.cancer.gov	CPTAC-5824
ARAF_NLGYRDS[+80]GYYWEVPPSEVQLLK_S299_immuno	assays.cancer.gov	CPTAC-5826
BRAF_GDGGSTTGLSATPPASLPGSLTNVK_immuno	assays.cancer.gov	CPTAC-5821
BRAF_GLIPEC[+57]C[+57]AVYR_immuno	assays.cancer.gov	CPTAC-5771
BRAF_RDSSDDWEIPDGQITVGQR_immuno	assays.cancer.gov	CPTAC-5820
BRAF_DSSDDWEIPDGQITVGQR_immuno	assays.cancer.gov	CPTAC-5818
BRAF_GDGGSTTGLSAT[+80]PPASLPGSLTNVK_T401_immuno	assays.cancer.gov	CPTAC-5822
BRAF_DS[+80]SDDWEIPDGQITVGQR_S446_immuno	assays.cancer.gov	CPTAC-5817
BRAF_RDS[+80]SDDWEIPDGQITVGQR_S446_immuno	assays.cancer.gov	CPTAC-5819
RAF1_GLQPEC[+57]C[+57]AVFR_immuno	assays.cancer.gov	CPTAC-5780
RAF1_GYASPDLSK_immuno	assays.cancer.gov	CPTAC-5778
RAF1_STSTPNVHMVSTTLPVDSR_immuno	assays.cancer.gov	CPTAC-5828
RAF1_VVDPTPEQFQAFR_immuno	assays.cancer.gov	CPTAC-5779
RAF1_STS[+80]TPNVHMVSTTLPVDSR_S259_immuno	assays.cancer.gov	CPTAC-5829
MAP2K1_ISELGAGNGGVVFK_immuno	assays.cancer.gov	CPTAC-5745
MTOR_DLELAVPGTYDPNQPIIR_immuno	assays.cancer.gov	CPTAC-5753
MTOR_IQSIAPSLQVITSK_immuno	assays.cancer.gov	CPTAC-5752
MTOR_LFDAPEAPLPSR_immuno	assays.cancer.gov	CPTAC-5755

(*Continued on next page*)

Continued

REAGENT or RESOURCE	SOURCE	IDENTIFIER
MTOR_LTESLDFTDYASR_immuno	assays.cancer.gov	CPTAC-5754
MTOR_TDSYSAGQSVEILDGVELGEPAHK_immuno	assays.cancer.gov	CPTAC-5797
MTOR_TRTDSYSAGQSVEILDGVELGEPAHK_immuno	assays.cancer.gov	CPTAC-5799
MTOR_TGTTVPESIHSFIGDGLVKPEALNK_immuno	assays.cancer.gov	CPTAC-5794
MTOR_TGTTVPESIHSFIGDGLVKPEALNKK_immuno	assays.cancer.gov	CPTAC-5796
MTOR_VLGLLGALDPYK_immuno	assays.cancer.gov	CPTAC-5756
MTOR_TDS[+80]YSAGQSVEILDGVELGEPAHK_S2448_immuno	assays.cancer.gov	CPTAC-5798
MTOR_TRTDS[+80] YSAGQSVEILDGVELGEPAHK_S2448_immuno	assays.cancer.gov	CPTAC-5800
MTOR_TGTTVPESIHS[+80]FIGDGLVKPEALNK_S2481_immuno	assays.cancer.gov	CPTAC-5793
MTOR_TGTTVPESIHS[+80] FIGDGLVKPEALNKK_S2481_immuno	assays.cancer.gov	CPTAC-5795
GSK3B_LLEYTPTAR_immuno	assays.cancer.gov	CPTAC-5749
GSK3B_TPPEAIALC[+57]SR_immuno	assays.cancer.gov	CPTAC-5750
GSK3B_TTSFAESC[+57]KPVQQPSAFGSMK_immuno	assays.cancer.gov	CPTAC-5790
GSK3B_VIGNGSFGVVYQAK_immuno	assays.cancer.gov	CPTAC-5751
GSK3B_TTS[+80]FAESC[+57]KPVQQPSAFGSMK_S9_immuno	assays.cancer.gov	CPTAC-5791
MAPK1_VADPDHDHTGFLT[+80]EY[+80]VATR_T185/ Y187_immuno	assays.cancer.gov	CPTAC-5812
MAPK1_VADPDHDHTGFLT[+80]EYVATR_T185_immuno	assays.cancer.gov	CPTAC-5809
MAPK1_VADPDHDHTGFLTEY[+80]VATR_Y187_immuno	assays.cancer.gov	CPTAC-5810
MAPK1_VADPDHDHTGFLTEYVATR_immuno	assays.cancer.gov	CPTAC-5811
MAPK3_ALDLLDR_immuno	assays.cancer.gov	CPTAC-5760
MAPK3_IADPEHDHTGFLTEYVATR_immuno	assays.cancer.gov	CPTAC-5813
MAPK3_IADPEHDHTGFLT[+80]EY[+80]VATR_T202/ Y204_immuno	assays.cancer.gov	CPTAC-5814
MAPK3_IADPEHDHTGFLT[+80]EYVATR_T202_immuno	assays.cancer.gov	CPTAC-5816
MAPK3_IADPEHDHTGFLTEY[+80]VATR_Y204_immuno	assays.cancer.gov	CPTAC-5815
FOS_APHPFGVPAPSAGAYSR_immuno	assays.cancer.gov	CPTAC-5783
FOS_GSSSNEPSSDSLSSPTLLAL_immuno	assays.cancer.gov	CPTAC-5781
FOS_TEPFDDFLFPASSR_immuno	assays.cancer.gov	CPTAC-5782
EGFR_GSHQISLDNPDYQQDFFPK_immuno	assays.cancer.gov	CPTAC-5831
EGFR_IPLENLQIIR_immuno	assays.cancer.gov	CPTAC-5785
EGFR_NLQEILHGAVR_immuno	assays.cancer.gov	CPTAC-5784
EGFR_YSSDPTGALTEDSIDDTFLPVPEYINQSVPK_immuno	assays.cancer.gov	CPTAC-5834
EGFR_Y[+80] SSDPTGALTEDSIDDTFLPVPEYINQSVPK_Y1045_immuno	assays.cancer.gov	CPTAC-5835
EGFR_YSSDPTGALTEDSIDDTFLPVPEY[+80] INQSVPK_Y1068_immuno	assays.cancer.gov	CPTAC-5833
EGFR_GSHQISLDNPDY[+80]QQDFFPK_Y1148_immuno	assays.cancer.gov	CPTAC-5832
EGFR_GSTAENAEY[+80]LR_Y1173_immuno	assays.cancer.gov	CPTAC-5830
ERBB2_GIWIPDGENVK_immuno	assays.cancer.gov	CPTAC-5777
ERBB2_GTPTAENPEY[+80]LGLDVPV_Y1248_immuno	assays.cancer.gov	CPTAC-5827
ERBB3_LTFQLEPNPHTK_immuno	assays.cancer.gov	CPTAC-5768
ERBB3_SLEATDSAFDNPDYWHSR_immuno	assays.cancer.gov	CPTAC-5766
ERBB3_YLERGESIEPLDPSEK_immuno	assays.cancer.gov	CPTAC-5767
CCND1_AC[+57]QEQIEALLESSLR_immuno	assays.cancer.gov	CPTAC-5761
CCND1_AEETC[+57]APSVSYFK_immuno	assays.cancer.gov	CPTAC-5764
CCND1_AYPDANLLNDR_immuno	assays.cancer.gov	CPTAC-5765
CCND1_FLSLEPVKK_immuno	assays.cancer.gov	CPTAC-5763

(*Continued on next page*)

CellPress
OPEN ACCESS

Continued

REAGENT or RESOURCE	SOURCE	IDENTIFIER
CCND1_VIKC[+57]DPDC[+57]LR_immuno	assays.cancer.gov	CPTAC-5762
RPTOR_ALETIGANLQK_immuno	assays.cancer.gov	CPTAC-5744
RPTOR_SYNC[+57]TPVSSPR_immuno	assays.cancer.gov	CPTAC-5743
FOXO3_AVS[+80]MDNSNKYTK_S253_immuno	assays.cancer.gov	CPTAC-5836
MAPK8_TAGTSFMMTPY[+80]VVTR_Y185_immuno	assays.cancer.gov	CPTAC-5792

RESOURCE AVAILABILITY

Lead contact

Further information and requests for resources and reagents should be directed to and will be fulfilled by the Lead Contact, Amanda Paulovich (apaulovi@fredhutch.org).

Materials availability

Antibodies for immuno-MRM assays have been deposited to the CPTAC Antibody Portal (antibodies.cancer.gov). Assay characterization data and protocols have been deposited to the CPTAC Assay Portal (assays.cancer.gov).

Data and code availability

The accession number for the data reported in this paper is Panorama: NmDXGW. Panorama Public (Sharma et al., 2014) is a database of targeted proteomics measurements; the link for this dataset is (https://panoramaweb.org/NmDXGW.url). Characterization data for assays are available in the CPTAC Assay Portal (assays.cancer.gov).

EXPERIMENTAL MODEL AND SUBJECT DETAILS

Cell lines

HCT-116 (ATCC catalog# CCL-247), HT-29 (ATCC catalog# HTB-38), A375 (ATCC catalog# CRL-1619), and SK-MEL2 (ATCC catalog# HTB-68) cells were grown in 150 mm TC plates in 30mL of DMEM/F12 supplemented with 10% FBS and treated with PLX-4720 at 48h, 24h and 1.5 h time points. PLX-4720 and DMSO controls were added in fresh media for every time point. After treatment, adherent cells were released in 0.25% trypsin and washed 3x with DPBS. Lysis buffer (6 M Urea, 25 mM Tris pH 8.0, 1 mM EGTA, 1 mM EDTA, Sigma phosphatase cocktail 1 and 2 and Sigma Protease inhibitor) was added to the pellet at 5 x 10^7 cells/mL. Cells suspended in lysis buffer were sonicated 3 times with a Qsonica Sonicator, Pulse 1 sec on and 1 sec off at 70% amplitude. Lysates were then spun at 20,000 x g for 15 min at 4°C. After confirming the common signaling pathways dysregulated after PLX-4720 treatment, the cell lines were scaled up, treated with PLX-4720 and the lysates shipped to FHCRC on dry ice for distribution to the three proteomics laboratories.

METHOD DETAILS

Proliferation assays

Cells were seeded at 1,000 cells/well in a 384-well black wall tissue culture plate (Greiner microClear®) in DMEM/F12 supplemented with 10% FBS. (For experiments in which media was changed, the cells were washed with DPBS 1X and supplemented with indicated media before drug treatment). Cells were treated with PLX-4720 and a final DMSO concentration of 0.25% 12–18 h after seeding. Plates and cells were harvested 72 h post treatment using CellTiter-Glo® Luminescent Cell Viability Assay (Promega: G7570) and read on Envision multimode Plate Reader (PerkinElmer). Relative viability was calculated as a percent change relative to 0.25% DMSO control treated wells.

Western blot analysis

HCT-116, HT-29, A375 and SK-MEL2 cells were seeded (300,000 in 3 mL DMEM/F-12 supplemented with 10% FBS) in a 6-well tissue culture plate and treated with PLX-4720 at 48h, 24h and 1.5 h time points. PLX-4720 and DMSO controls were added in fresh media for all time points. After treatment cells were collected and lysed using lysis buffer (1% Triton X100, 20 mM Tris pH 7.5, 50 mM NaCl, 2 mM $MgCl_2$, 1mM EDTA, and EGTA and Halt protease and phosphatase inhibitors). The membranes were immunoblotted using primary antibodies overnight, incubated with LI-COR secondary antibodies for 45 min, and scanned on Odyssey® CLx Imaging System.

Peptide selection criteria

Using the existing cancer biology literature and proteomics resources, each of these targets was comprehensively reviewed. First, existing LC/MS proteomic datasets (including data from breast, ovarian, and colorectal cancer tissues, cancer cell lines, and public

databases) were mined for empirical evidence of detection of corresponding peptides. For modified targets, datasets incorporating phosphopeptide enrichment were used for searching. Each dataset was searched for matching peptides to the gene product identified on the master list, or in the case of post-translationally modified targets, the datasets were searched for the tryptic sequence containing the modification (searches allowed for identifications encompassing missed trypsin cleavage sites). Selected peptides were required to be proteotypic (i.e., unique to the protein target of interest and featuring a good response by mass spectrometry) and were prioritized by frequency of observation, MS intensity, length (between ~7-25aa), hydrophobicity (10-40 by SSRCalc) or retention time, charge state (z=2,3), amino acid composition (deprioritize M, N-terminal Q, N-terminal C, multiple P, previous and next amino acids containing trypsin sites (ie. ragged ends)), and frequency of missed cleavage products. After ranking of the peptides based on those criteria, further review focused on a peptide-level knowledge of biology, which included known sites of mutation using CBioPortal (Cerami et al., 2012), post-translational modifications using PhosphoSitePlus (Hornbeck et al., 2012, 2019), and assessment of potential interference using the *in silico* Peptide Interference Predictor (Remily-Wood et al., 2014).

Enzymatic digestion

Cell lysates were analyzed in a blinded fashion. Lysates were diluted to 2 mg/mL with lysis buffer. Aliquots were transferred to 2 mL deep-well plates and sealed with pierceable film. Reduction was performed by addition of 0.5 M triscarboxyethylphosphine (TCEP) and incubated for 30 min at 37°C with mixing. Cysteines were alkylated with iodoacetamide for 30 min in the dark. To decrease urea concentration, 0.2 M Tris (pH 8.0) was added to decrease urea concentration to ~0.6 M prior to addition of Lys-C at a 1:50 enzyme: substrate ratio. The mixture was incubated for 2 h at 37 °C with mixing, followed by addition of trypsin at a 1:50 enzyme: substrate ratio. The mixture was incubated overnight (16 h) at 37 °C. Formic acid (aqueous 20% v/v) was added to quench the digestion at a final acid concentration of 1%. The heavy SIS peptide master mix was added to the digested peptides prior to desalting. The digested peptides were desalted on SPE plates by equilibrating with 1% formic acid, loading the peptide mixture on the plates, washing 3x with aqueous 0.1% formic acid, and elution with aqueous 50% acetonitrile/0.1% formic acid. Eluted peptides were lyophilized to powder.

Peptide immunoaffinity enrichment

Custom rabbit and mouse monoclonal antibodies were crosslinked to Protein G agarose magnetic particles (GE Healthcare). The dried peptides were resuspended in PBS/0.01% CHAPS in 96 well plates and adjusted to pH 8.0 with 1 M Tris. 24 μL of antibody beads (corresponding to panel mix #1; monoclonal antibodies to phosphorylated peptides crosslinked to Protein G beads) was added to the solution, the plate was sealed, and samples were incubated overnight at 4 °C with tumbling on a Labquake tube rotator or Lab Shaker. Following incubation, the plates were centrifuged at 800 × g for 30 seconds and processed using a KingFisher automated magnetic particle processor. The beads were washing twice with PBS/0.01% CHAPS and once with 0.1X PBS/0.01%CHAPS. The peptides were eluted from the beads with aqueous 3% acetonitrile/5% acetic acid / 50mM citrate. The flow-through was used in a sequential enrichment experiment by adding antibody beads (corresponding to panel mix #2; monoclonal antibodies to unmodified peptides crosslinked to Protein G beads) and repeating the enrichment procedure as described above.

Liquid chromatography multiple reaction monitoring mass spectrometry

Direct-MRM and IMAC-MRM LC-MS was performed with a Dionex Ultimate 3000 RS system coupled to a Thermo Quantiva triple quadrupole mass spectrometer. Peptides were loaded on a trap column (Acclaim Pepmap 100 C18, 20 mm x 100 μm) using mobile phase A (0.1% formic acid in 2% acetonitrile). The LC gradient was delivered at 300 nL/minute and consisted of a linear gradient of mobile phase B (90% acetonitrile and 0.1% formic acid in water) developed on a 25 cm x 75 μm column (Acclaim Pepmap C18, 2 μm particles) from 2%–8% B in 1 minute, 8%–26.5% B in 41.5 minutes, 26.5%–50% B in 6 minutes, 50%–90% B in 30 seconds, 90%–96% B in 5.5 minutes, and re-equilibration at 2% B for 15 minutes. The nano electrospray interface was operated in the positive ion MRM mode. Parameters for collision energy (CE) were taken from optimized values in Skyline (MacLean et al., 2010). Q1 resolution was 0.4, Q3 resolution was 0.7. Immuno-MRM measurements were performed at two additional sites. The first site used a Proxeon Easy nLC-1000 system coupled to a Thermo Quantiva triple quadrupole mass spectrometer. Peptides were loaded using mobile phase A (0.1% formic acid in 2% acetonitrile) and 2% mobile phase B. The LC gradient was delivered at 200 nL/minute and consisted of a linear gradient of mobile phase B (90% acetonitrile and 0.1% formic acid in water) developed on a 15 cm x 75 μm column (Reprosil C18, 1.9 μm particles) from 2%–6% B in 2 minutes, 6%–30% B in 45 minutes, 30%–60% B in 6 minutes, 60%–90% B in 1 minute, and 5 minutes at 90%B. The final site used an Eksigent 425 nanoLC system with a nano autosampler and chipFLEX system (Eksigent Technologies, Dublin, CA) coupled to a 5500 QTRAP mass spectrometer (SCIEX, Foster City, CA). Peptides were loaded on a trap column (Reprosil C18, 5 mm x 200 μm) at 5 μL/min for 3 minutes using mobile phase A (0.1% formic acid in water). The LC gradient was delivered at 300 nL/minute and consisted of a linear gradient of mobile phase B (90% acetonitrile and 0.1% formic acid in water) developed from 3%–14% B in 1 minute, 14%–34% B in 20 minutes, 34%–90% B in 2 minutes, and re-equilibration at 3% B on a 15 cm x 75 μm chip column (ChromXP C18 particles, 3 μm). Scheduled MRM transitions used a retention time window of 150 seconds and a desired cycle time of 1.5 seconds, enabling sufficient points across a peak for quantitation. A minimum of two transitions (four total per peptide pair, including endogenous and spiked heavy peptides) were recorded for each light and heavy peptide. MRM data were analyzed by Skyline. Peak integrations were reviewed manually, and transitions from analyte peptides were

confirmed by the same retention times of the light synthetic peptides and heavy stable isotope-labeled peptides, and with equivalent relative areas of recorded transitions. Transitions with detected interferences were not used in the data analysis.

Fit-for-purpose assay validation

The analytical performance of the assays was characterized in response curves, repeatability, and inter-laboratory experiments. Response curves were generated in a background of cell lysates from the following cell lines (relative contribution in parentheses): MCF10A-EV (5), T47D (1.25), CCRF-CEM (1), COLO205 (2), COR-L23 (2.5), H2444 (3), H2122 (3), H1792 (1.25), HEPG2 (2), K-562 (1.25), and H226 (3.75) cells. The pooled lysate was digested (Lys-C + trypsin) and heavy SIS peptides added by serial dilution (heavy spike amounts (fmol): 2000, 200, 20. 8, 3.2, 1.28, 0.512, 0.2048). Light peptide was added at a constant concentration (light spike (fmol): 50 (phosphopeptides), 20 (nonmodified peptides)). Blanks were prepared by using background lysate spiked with light peptide and no heavy peptides. All points were analyzed by immunoaffinity enrichment and MS in triplicate. Curves were analyzed using Skyline (MacLean et al., 2010) with a linear regression in log space with no weighting on all points above the lower limit of quantification. The Lower Limit of Quantification (LLOQs) was obtained by empirically finding the lowest point on the curve that had CV < 20% in the curve replicates. The upper limit of quantification (ULOQ) was determined by the highest concentration point of the response curve that maintained the linear range ($R^2 > 0.9$) of the response. For curves that maintained linearity at the highest concentration measured, the ULOQ is a minimum estimate.

Repeatability was determined by spiking heavy peptides at three concentrations (Low, Medium, High; spike levels (fmol) 2, 20, 200 (nonmodified); 5, 50, 500 (phosphorylated)) into the same pooled background lysate used in the response curves. Complete process triplicates (including digestion, enrichment – if applicable, and MS) were prepared and analyzed over five days. Intra-assay variation was calculated as the mean CV obtained within each day. Inter-assay variation was the CV calculated from the mean values of the five days. All replicates included in the repeatability calculation were required to be above the LLOQ determined from response curves.

Inter-laboratory validation was conducted using the immuno-MRM assays in three independent laboratories using a "mini-kit" approach: a common set of antibodies linked to beads and master mixes of synthetic peptides were prepared centrally and distributed to participating sites. Response curves and repeatability experiments were run independently at each site to determine respective performance figures of merit. Inter-laboratory validation was conducted on lysates from the cell line samples used in proof-of-principle demonstration studies. As described above, lysates were prepared centrally and shipped to participating sites for analysis (i.e., digestion, enrichment, and MS was performed independently at each site). Due to differences in detection efficiency of some peptides at sites (different instruments and operating conditions), validated assays were required to be characterized at least two of the three sites.

Data analysis

Peak integration was performed in Skyline (MacLean et al., 2010). Specificity was determined by consistent retention times of light and heavy peptides in addition to relative intensity of transitions in light and heavy peptides within 30% of mean values. Integrated raw peak areas were exported from Skyline and total intensity was calculated using Peak Area + Background. Peak area ratios were obtained by dividing peak areas of light peptides by that of the corresponding heavy peptides and ratios were log (base 2) transformed for heat maps and statistical analysis. Immuno-MRM results from site 1 were used for data analysis except for peptides below LLOQ in a majority of samples, in which data from site 2 or 3 data were used (where possible).

QUANTIFICATION AND STATISTICAL ANALYSIS

Statistical analysis was performed using R and Microsoft Excel. Details for statistical analysis can be found in the figure legends.